INFORMATION TO USERS

This manuscript has been reproduced from the microfilm master. UMI films the text directly from the original or copy submitted. Thus, some thesis and dissertation copies are in typewriter face, while others may be from any type of computer printer.

The quality of this reproduction is dependent upon the quality of the copy submitted. Broken or indistinct print, colored or poor quality illustrations and photographs, print bleedthrough, substandard margins, and improper alignment can adversely affect reproduction.

In the unlikely event that the author did not send UMI a complete manuscript and there are missing pages, these will be noted. Also, if unauthorized copyright material had to be removed, a note will indicate the deletion.

Oversize materials (e.g., maps, drawings, charts) are reproduced by sectioning the original, beginning at the upper left-hand corner and continuing from left to right in equal sections with small overlaps. Each original is also photographed in one exposure and is included in reduced form at the back of the book.

Photographs included in the original manuscript have been reproduced xerographically in this copy. Higher quality 6" x 9" black and white photographic prints are available for any photographs or illustrations appearing in this copy for an additional charge. Contact UMI directly to order.

UMI®

Bell & Howell Information and Learning
300 North Zeeb Road, Ann Arbor, MI 48106-1346 USA
800-521-0600

Thermally Stable ZSM-5 Zeolite Materials With New Microporosities.

David Ohayon

A Thesis

in

The Department

Of

Chemistry and Biochemistry

Presented in Partial Fulfillment of the Requirements
for the Degree of Master of Science at
Concordia University
Montreal , Quebec , Canada .

December 1998

Abstract

Thermally Stable ZSM-5 Zeolite Materials With New Microporosities.

David Ohayon

The desilicated forms of the Na-X , Na-Y , the ammonium and sodium forms of the ZSM-5 zeolite were prepared by a process which involves the selective removal of silicon atoms from the parent zeolite in an aqueous basic solution . This treatment has the effect to decrease the Si/Al ratio while keeping the zeolite structure almost unmodified . In all cases ,we noticed an enhancement of the ion-exchange capacity . This property could be exploited industrially since the desilicated forms have higher total ion removal rates of calcium and magnesium ions from a solution of hard water .

As for two ZSM-5 zeolites ,having quite different Si/Al ratio , the preparation of highly thermally stable zeolite materials with smaller micropores at 4.9 Å or larger at 5.5 Å than those of the parent ZSM-5 zeolites was possible . These final materials were obtained by a process which involved the following additional steps : i) reinsertion into the desilicated ZSM-5 zeolite of a well defined amount of silicon species (sodium orthosilicate and pyrosilicate) which have been selectively removed from the zeolitic framework during the desilication process, and

then ii) activation of the resulting materials in air at high temperatures(550 ^{0}C). The amount of the reinserted silicon containing species depends on the pore size wanted. The zeolite materials so obtained still have quite high surface areas and pore volumes .

This method has the great advantage of being very reproducible , giving us a micropore size which is much smaller or much larger by ± 0.4Å than the size of the parent zeolite with a quite homogeneous micropore distribution , and the latter characteristic must result in selectivity in catalysis or adsorption .

Dedicated

To my Parents and all of
my Family for their love .
All the teachers I have had
and to whom I owe so much.

Acknowledgments

I would like to express my sincere appreciation and gratitude to Professor Raymond Le Van Mao for his advice , support , patience and encouragement throughout all parts of my research work .

I would also like to thank :

Drs. O.S. Tee , M. Lawrence and L.Coolebrook as my committee members for their time and very valuable suggestions ;

Tuan S. Le for teaching many useful techniques used in the laboratory and his valuable friendship.

Dr. Patterson and Tran Tan for their assistance in the field of Atomic Absorption .

Office staff , in particular , Ms. C.J. Coutts for the assistance and help when needed .

The many French students that have come and gone over the past 3 years , always leaving good souvenirs behind .

Cecilia Madamba and Muntassar for their friendship and assistance with the XRD instrument .

All my friends in the department , especially my tea partner Ms.Sourial and her partner in crime Ms. Peres , without them things would have not been the same .

Finally , I wish to express my deepest gratitude to my parents for their love , moral support and understanding . Without them , this work would have never been accomplished .I would also like to thank my brother Michael for his support and never taking me too serious in my stressful moments .The last person I would like to thank and not the least is Ms. S.Benguira for her encouraging words that always lifted my spirits , her love and her total understanding of what I was going through , I will never forget it .

TABLE OF CONTENT

List of Figures

Chapter 2

Chapter 3

Chapter 4

APPENDIX

List of Tables

Chapter 2

Chapter 4

Chapter 1

1.1 Literature Review on Pore Size engineering in Zeolites .

The modification of the zeolites' pores is a very important tool for various purposes such as in the separation of gas mixtures , ultra purification of gases and the storage and transport of unstable , dangerous or explosive gases .

The separating ability of zeolites can be achieved or altered by the molecular sieving caused by size and/or shape differences between the zeolitic crystal aperture and the adsorbate molecule . In addition, selectivity can be caused by differences in the interaction energies between the adsorbate molecules in a specific zeolite .

Molecular Sieving Effect

i) The first modification method is by cation exchange process . This works by changing the exchangeable cation in a zeolite which may enlarge or narrow the pore openings by diminishing the cation diameter .With zeolite A, divalent ion-exchange opens the aperture to full diameter , whereas exchange

exchange with a larger univalent ion diminishes the opening's size . It has been shown that the pore reduction does not occur gradually with increasing extent by exchange but rather suddenly at a level of about 25 % potassium exchange as mentioned by Breck .[1]

ii) The second modification involves the preadsorption of polar molecules . Small amounts of polar molecules such as water or ammonia are preadsorbed in a dehydrated zeolite , and the adsorption of a second adsorbate can be drastically reduced . It has been shown that for Zeolite A , there is a strong interaction between the zeolite's cation and the dipole moment of the polar molecules which produce a diffusion block by clustering the polar molecules around the exchangeable cations in the zeolite channels .

iii) The last modification is of the zeolitic framework . The pore size engineering can be achieved by a modification of the zeolitic framework resulting from 1 of these 3 techniques : 1) the first technique involves modification by crystallographic changes where the molecular sieve behavior of zeolites can be controlled by a hydrolytic process at elevated temperatures because of cationic migration . The water vapors which are in contact with the zeolite crystals at high temperatures result in a variation of the zeolitic adsorption characteristics . The amount of water vapor , pretreatment

temperature and the pretreatment time can control the effective pore size of zeolites . 2) The second technique for pore size modification results of an internal and external modification by the implantation of additional groups in the zeolitic pores . The methods to vary the pore systems are : 1) silanation , 2) disilanation , 3) boranation , 4) implantation of boron-nitrogen compounds and 5) modification by inorganic acids and their salts .[2]

The third technique comes from a paper entitled " Production of Porous Materials by Dealumination of Alumina-Rich Zeolites " by Le Van Mao et al. .[3] They talked about a method that would enable us to get larger pores . This process used ammonium hexafluorosilicate (AFS) on an alumina rich zeolite such as Ca-A . They started with an initial diameter of 1.7 nm and got larger mesopores after treatment which were in the region of 12 nm with fairly narrow peaks which suggest homogeneous pore sized systems with much higher void volumes . The authors then did a comparative study using the Na-X zeolite which has a higher Si/Al ratio with a diameter smaller than 1.7 nm . They found that after treatment mesopores of about 4 nm were obtained and they got a sharper and narrower pore size distribution than for the Ca-A/AFS treated sample . This could be explained by the fact

that having a high Si/Al ratio prevented any serious damage to the zeolite pore system and so increased the pore openings of the treated Na-X only slightly compared to the treated Ca-A sample .

A mild and controlled dealumination of alumina rich zeolites will give us mesoporous materials with fairly homogeneous pore systems . Several advantages are associated with the AFS treatment which are : 1) having only slightly diminished cation exchange properties , 2) having higher void volumes in the case of alumina-rich parent A zeolites and 3) having high thermal stabilities .[3]

As the catalytic reactions are concerned , selectivity in adsorption and reaction can be investigated by several techniques as shown by Forni [4] in a paper on the "Standard Reaction Tests For Microporous Catalysts Characterization " . In it he discusses the fact that the choice of molecular sieves as dimensionally selective catalysts require an as rapid as possible collection of reliable information on the porous structure of such materials . The information could be obtained by using either crystalline structure or selectivity of adsorption of some properly selected probe molecules .We know that the active sites are located within the pores , so the probability for the reactants to penetrate inside the pores and react depends on the pore size

and the structure of the reacting molecules because the molecules need to be small enough to enter but also the molecules which are small enough will be able to diffuse out of the pores as products . Several types of selectivity have been accepted , they are : 1) Reactant Selectivity , 2) Product Selectivity , 3) Reaction Intermediate Selectivity and 4) Molecular Traffic Control Selectivity .

The distribution of the reaction products in properly chosen simple test reactions , exploiting the acidic properties of the catalyst , makes it possible for them to define the value of some characteristic parameters , such as the constraint index (CI) . To get information on the pore structure of a catalyst we have to compare its selectivity in a given set of probe- reactions with that measured on known catalysts for the same reactions . Comparing the cracking of an equimolar mixture of n-hexane (nH) and 3-methyl-pentane (3MP) on acidic zeolites he noticed that there was a change in the cracking rate of the two paraffins due to the steric hindrance of the reaction intermediate . The ratio of the pseudo-first order cracking rates ($K_{nH}/K3_{MP}$) at a given temperature and for a given strength of acid sites is the constraint index . It grows with decreasing pore diameter and in the presence of small amounts of

noble metals in the catalyst .

The modified constraint index (CI^*) changes with the load of noble metal , so if for example we increase the platinum weight (%) then that will decrease the CI^* and the actual pore size of the catalyst becomes lower at high platinum loading . Another characteristic parameter is the spaciousness index (SI) . In the reaction that involved the cracking of butyl-cyclohexane (BCH) , the measurement of the (iso-butane/n-butane) yield ratio was very easily measurable and it grew with increasing pore size of the catalyst . This is referred to as the spaciousness index , and it is virtually independent of reaction conditions severity and it is a sensitive parameter for analysing the typical pore size of 12 membered ring zeolites .

These parameters permit us to clearly distinguish the behaviour of small - , medium- and large-pore microporous materials in catalytic reactions, the pore diameter of which can easily be ranked on the basis of a very few or even of only one test reaction .[4]

1.2 Objectives Of the Research Work

Our objective was to develop a unique procedure for enlargement or narrowing of the zeolite micropores which would be simple , predictable , reproducible and applicable to a large number of zeolites or other crystalline silicates . The chemical constituent of these materials involved in this process is silicon . It is known that zeolite pore size engineering can be done in many fashions , in particular by deposition of silicon or phosphorous compounds resulting thus in pore mouth narrowing , or by dealumination of alumina rich zeolites leading to an enlargement of the micropores .Reports in the literature indicate that this could be somewhat successful for low Si/Al ratio zeolites but ZSM-5 has a Si/Al ratio close to 20 and this method would not work due to the small amount of alumina it contains. According to our working hypothesis , pore size can be modified by a stepwise procedure which includes desilication (selective removal of silicon) and framework stabilization by thermal treatment . The latter can eventually be preceded by partial reinsertion of the removed silicon species .

The whole method bears the name of **DRS** which stands for **D**esilication , **R**esilication and **S**tabilization . One aspect of larger pore sizes is : shape selectivity , which may affect significantly the adsorptive ,

diffusive , catalytic or ion-exchanging properties of molecular sieves , when compared with the parent zeolites or with amorphous or mesoporous materials . One of the possible applications with this method would be as an additive to the fluid cracking catalyst (FCC) which would be able to shift the spectrum of production from light olefins such as ethylene , propylene for narrower pore sizes to propylene, isobutene and other higher olefins for larger pore sizes .

1.3 Organization of the Thesis

The thesis is divided into five chapters . In chapter 1 , the literature review which is related to the subject of this thesis has been reviewed briefly. The objective of the research has also been elaborated in this section .

The background regarding the properties of the zeolites is included in chapter 2 as well as some theory on aspects of this research. The experimental details are given in chapter 3 . The results and discussion of the thesis are presented in chapter 4 . Finally in chapter 5 , we have the conclusion and suggestions for future works .

Chapter 2

INTRODUCTION

2.1 Heterogeneous Catalysis

Catalysts serve to reduce energy barriers associated with a reaction that is thermodynamically feasible by providing an alternative pathway of lower activation energy . They alter the rate of a reaction without affecting its free energy since the ratio of the activities of the product and the reacting species is unaffected , so that there is a minimum expenditure of energy . Historically , it was thought that these catalysts emerged unchanged after altering the reaction rate , but developments in the ability to observe surfaces at an atomic level have demonstrated that there are changes in the topology and even composition brought about by catalytic activity . Catalysts have a tendency to become sintered , etched , eroded or covered with residues left behind by the interacting molecules .[5]

A catalyst could be defined as a substance that increases the rate of approach to equilibrium for a chemical reaction without substantially being consumed in the process [5] . Figure 2.1 shows the changes in energy associated with a simple exothermic reaction . The velocity of a catalyzed

reaction for the conversion of reactants A and B into product P may be expressed as :

$$- d[A] / dt = K [A]^n [B]^m \quad (1)$$

where : [A] , [B] are the concentrations for reactants A and B . The terms n and m are the partial orders with respect to reactants A and B .

$$K= A \exp (-E \text{ hom.} / RT) \quad (2)$$

where : T is the temperature and R is the gas constant .E hom. is the activation energy for the homogeneous reaction , E ads. represents adsorption of the reactants onto the catalyst , E cat. is for the formation of the activated complex and E des. for the desorption of the products ; λ ads. is the enthalpy of adsorption of the reactants and is taken to be exothermic ,and λ des. being the enthalpy of desorption of products is taken to be endothermic . The reaction rate at a given temperature will be increased by finding some means of reducing E hom. or increasing the preexponential factor A in equation (2) . In the presence of a catalyst , which might chemisorb A or B or both , the system may follow an alternative reaction path of lower energy of activation E cat. . Here the system appears to pass through a new chemisorbed transition state. The overall energy change upon reaction is ΔH and is the same for the two pathways [5] .

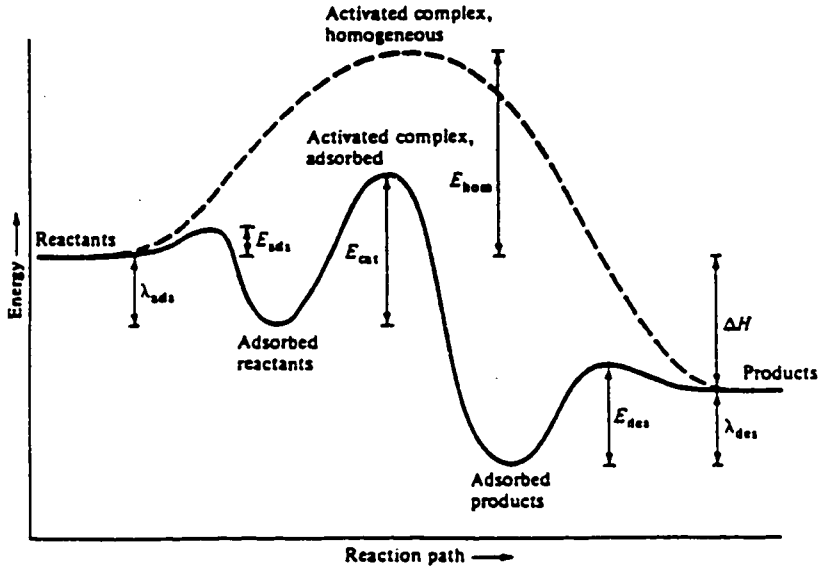

Figure 2.1 Energy changes associated with individual steps of a chemical reaction.

2.2 Catalyst Technology

2.2.1 From the Perspective of Petroleum Refining

Catalytic technology forms the backbone of the chemical and petroleum industries since many of the synthetic and refining processes are catalytically controlled . There is a major push to continue technological advancements in the field of catalysis and the progression of catalytic developments continue .The major goal of a catalyst researcher is to develop novel catalysts for already existing processes , then to optimize the various components in their complementary role with respect to activity and selectivity with emphasis on the minimization of the energy consumed and the pollution .

It is necessary to understand the processing of any catalytic reaction at an atomic level and to discover the mechanism by which catalysis proceeds so that one can design and construct the most efficient catalyst for a particular reaction . How successful a catalyst is , depends on its ability to reduce the activation energy barrier for a reaction . Another approach is to develop a means of reducing energy consumption to effect the same results of a more efficient catalyst . Advanced surface analysis techniques are a key element for successfully developing and characterizing catalysts . The advantage of

performing analysis in situ is obvious if one considers the possible variations in catalytic behavior that actual conditions incur compared to empirically optimized reaction conditions . The optimization of each parameter is directly controlled by the operator and can be manipulated in the desired fashion and the effects monitored . Under typical reaction conditions, however, the extent to which one can exert control over the reaction is limited . [6]

2.2.2 Zeolites Structures

Zeolites are porous , crystalline aluminosilicates containing cavities and channels of molecular dimensions ranging from 3 to 10 Å .

The general formula of a zeolite is :

$$Me_{x/n}^{n+} * [(AlO_2)_x^- * (SiO_2)_y] * m H_2O \quad (2)$$

where : Me^{n+} is the cation that satisfies the electrical neutrality of the structure .

The primary building block of the zeolite structure is a tetrahedron of four oxygen atoms surrounding a central silicon atom , $-(SiO_4)^{4-}$, or an aluminum atom $-(AlO_4)-^{5-}$ as illustrated in fig.2.2 a) . By joining these tetrahedra together through shared apical oxygen atoms , a secondary building unit is produced, that of fig. 2.3 b) . These are interconnected to form a polyhedra as in fig. 2.3 c) which in turn connect to form the infinitely extended frameworks of the various specific zeolite crystal structures of fig. 2.3 d) , in which the corners of the polyhedra represent Si or Al atoms and the connecting lines are the shared oxygen atoms . [7]

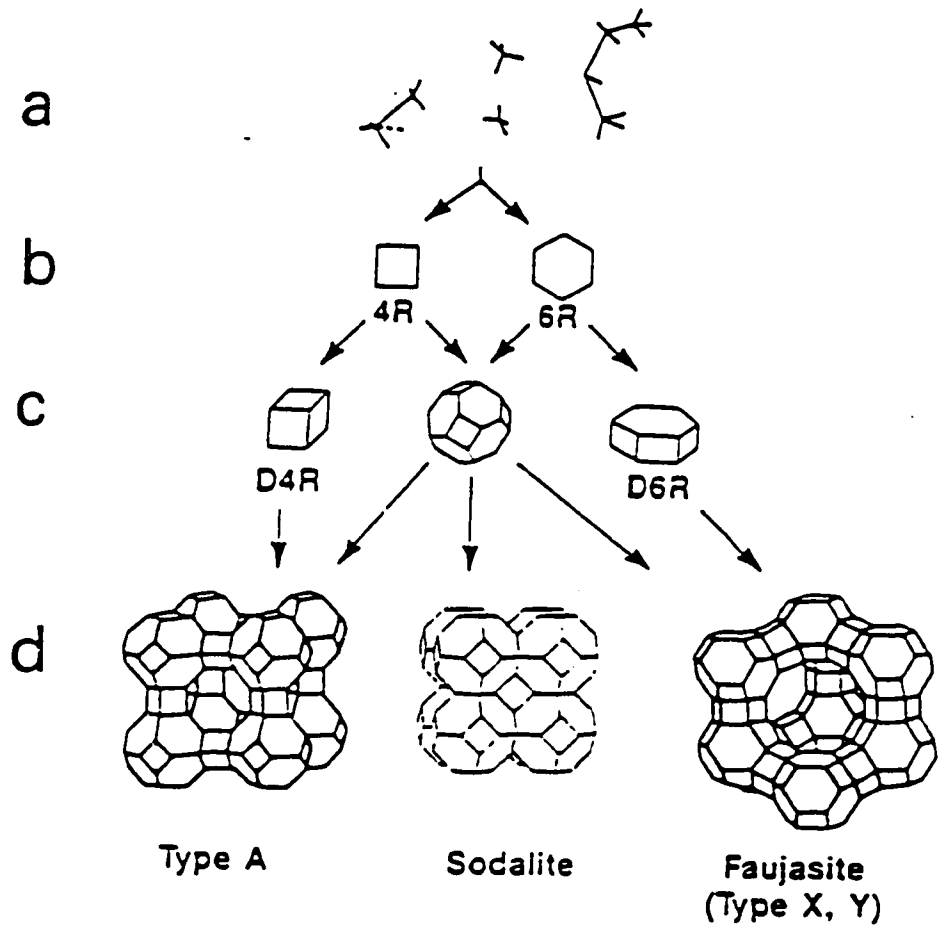

Figure 2.2 The production process of a zeolite structure . a)Primary units , b)Secondary units , c) Tertiary unit (building polyhydron) , d)Zeolite structures .

In nature we find 34 different known types of zeolites and among those of interest as catalysts , a few are found in abundance . The ability of researchers to synthesize zeolites of known and new structures in the laboratory has led to new discoveries . Up to date , nearly 100 synthetic zeolites have been identified , having a large variety of different framework structures with pore openings ranging from less than 5 Å to greater than 10 Å . [8,9]

2.2.3 Zeolite as Catalysts

The use of zeolites as commercial cracking catalysts was first announced in 1960 . By 1976 , it was estimated that this development saved the petroleum industry and ultimately the U.S public more than 3 billion dollars in reduced petroleum and refining costs compared to using the previously used silica-alumina catalysts . [10,11]

Zeolites have long been used for water softening , utilizing their ion-exchange capacities , and for drying . Beside their large scale use as industrial catalysts in petroleum refining and chemical manufacture , zeolites have evolved as environmental catalysts in auto emissions control [12,13,14] , detergent (non-phosphate) builders [15] , selective adsorbents , membrane synthesis [16] and as modifiers at electrode surfaces in electrochemical applications . [17,18,19]

2.2.4 Properties of Zeolites

One of the most important properties of zeolites is their ability to exhibit shape selective catalysis [20] . Their ability to combine molecular sieving properties with unusually high activity for acid catalyzed reactions such as cracking and dehydration make them especially interesting . Their

pore diameters vary between 3 and 8 Å and their pore sizes usually fall within a discret range with a narrow pore size distribution . Since most catalytic sites are located within the pores of the catalysts , the relative probability of forming product molecules depends on the accessibility of reactant molecules to the active sites . Other properties which render them efficient catalysts are their high internal surface area , usually well over 300 m^2/g depending on the zeolite , and the presence of ion-exchangable cationic sites which allow the introduction of various metal cations with variable catalytic properties . Replacement of a metal cation with a proton (H^+) generates strong acid sites which are at the origin of catalytic activity in solid acidic catalysts . [19]

2.2.5 High Surface Area

The rate of a catalytic reaction is proportional to its active surface area .[20] Because of the high degree of porosity and their multichannel structure , zeolites exhibit extremely large internal surface areas relative to their external surface area . This is a major factor contributing to their efficiency as catalysts , since it will provide a greater accessibility of reactant molecules to the active sites where the reactions occurs . Occasionally a high surface area at the interface arises when 2 phases are coupled together under pressure leading to a contact synergy , thereby increasing the overall catalytic activity . [21,22]

Table 2.1 Typical Surface Areas of Common Zeolites

Zeolite	Surface Area (m^2/g)
ZSM-5	300-400
A	650
Beta	400-500
X and Y	700
MCM 41	>1000

2.2.6 Diffusion in Zeolites

Pore diameter in molecular sieves usually depends on the number of tetrahedra in the ring . The actual pore size is dependant on the type of cation present . Cations occupy positions which block part of the pores and adsorption inside them cannot occur until the adsorbate molecules are small enough to move freely into and within the pores [6] . When the molecules in the pore are nearly the size of the passageway , the diffusing molecules are never away from the influence of the wall , and the rate of diffusion becomes relatively slow . This has been variously termed restricted diffusion or configurational diffusion . In contrast , Knudsen diffusion occurs in pores sufficiently small that the mean free path is much greater than the pore size , but sufficiently larger than molecular motion which occurs by free flight interrupted by momentary adsorption and desorption on the wall . We could see the qualitative representation of the diffusion in the pores of solids as shown in fig.2.3 .

We have to note that diffusion in zeolites is more complex than Knudsen diffusion or bulk diffusion and the activation energy is usually much greater than that for Knudsen diffusion or bulk diffusion . [24]

Some typical reported values of diffusivities at 350 ^{0}C in ZSM-5 for p-

xylene , o-xylene and mesitylene were > 10^{-7} , 10^{-10} and 10^{-12} cm^2/s respectively . [24]

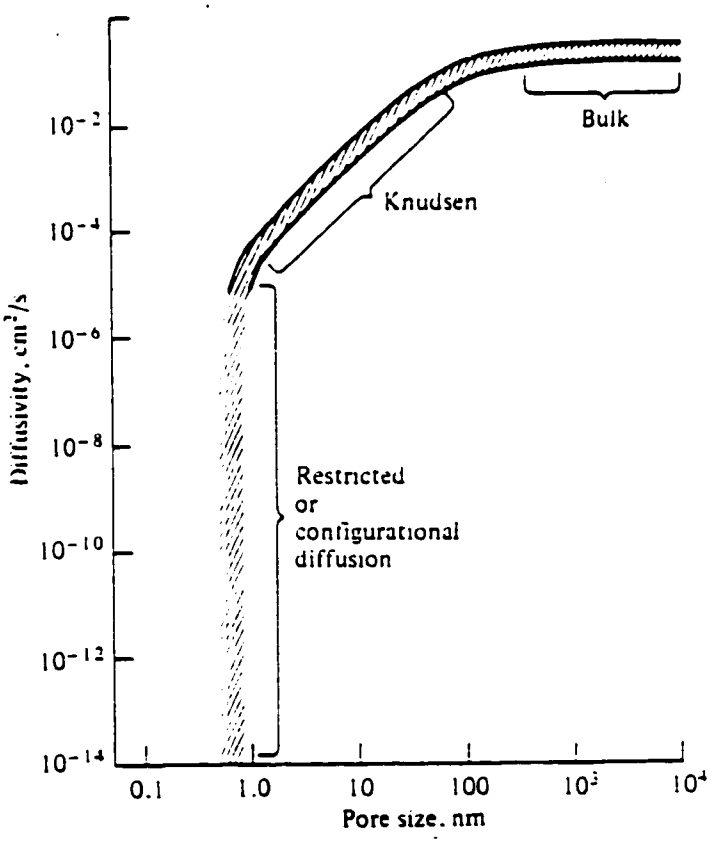

Figure 2.3 Effect of Pore size (nm) on Diffusivity(cm^2/s) .

2.2.7 Shape Selectivity

High crystallinity and regular pore structures and sizes are among the properties which render to zeolites their greatest advantages over other catalysts. Because of their specificity and selectivity for certain reactions and their ability to discriminate and exclude undesirable reactions from occuring , they achieve very high yields of particular products . It is possible to distinguish four different types of shape selectivities based on decreased diffusivity of either reactant or product molecules , which ultimately diminishes the reaction rate of the formation of the product . First , certain reacting molecules may be excluded from diffusing into the zeolite pores and are thus unable to gain access to the active sites because of pore limitations (fig. 2.4 a)) , a type of molecular exclusion known as reactant selectivity . Alcohol dehydration which requires weak acid sites is a typical case of reactant shape selectivity where secondary alcohols are excluded from the narrow pores of Ca-A zeolite . Secondly , if the product molecules formed are too bulky to freely diffuse out of the pores and into the surrounding media limiting the formation of certain products , it leads to the phenomena of product selectivity (fig. 2.4 b)) . The trapped products are either converted into less bulky products or they deactivate the catalyst by blocking its pores .

A very good example is the methylation of toluene for which the ortho and meta products are formed depending on the pore size of the catalyst . The third situation which arises is the formation of transition states which are restricted in movement by the size of the pores of the zeolite . This is a kinetic effect arising because of the local environment around the active site . Since neither reactant nor product molecules are prevented from diffusing through the pores , only the formation of the transition state is hindered . This is termed "restricted" transition state selectivity or spatio selectivity (fig. 2.4 (c)) . An interesting example is the acid catalyzed transalkylation of dialkyl benzenes.

The fourth situation is a type of molecular traffic control which may occur in zeolites with more than one type of pore system such as ZSM-5 . Reactant molecules may enter through one pore system and product molecules diffuse out through another (fig. 2.4 (d)) . In this way counter diffusion is minimized . This is illustrated in the alkylation of toluene over a modified ZSM-5 zeolite . [19]

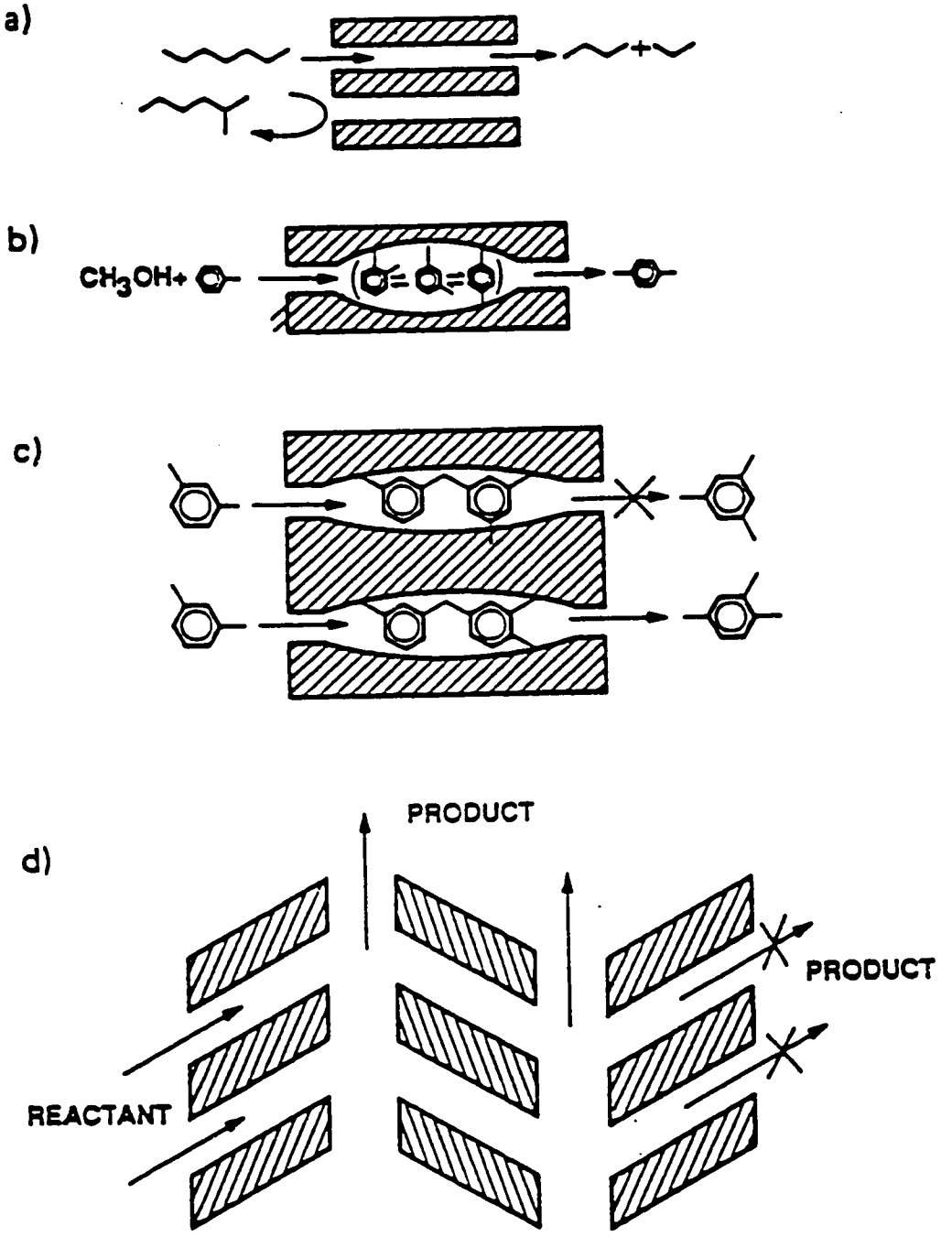

Figure 2.4 Shape Selectivity of zeolites (a), (b), (c) and (d) .

From fig. 2.5 , we can see the correlation between the effective pore size of various zeolites in equilibrium adsorption over temperature of 77 K to 420 K , with the kinetic diameters of various molecules from the Lennard Jones potential relation (see table 2.2) .

The contribution of the external surface of a zeolite crystal to its overall catalytic activity has often been questioned . With crystals larger than 1 micron , their external surface area relative to their intracrystalline surface area is so small (< 1%) that surface activity can be ignored . However , for small submicron crystals , external surfaces sites could be a significant fraction of the total surface area . If the external surface sites are catalytically either the same or more active than the intracrystalline sites , then shape selectivity of a zeolite could conceivably be changed by these surface sites . One such speculation was advanced by Frankel [21] who proposed the acid sites located in the "half cavities " or the external crystal surface of ZSM-5 could be active for a second type of shape selective reaction . These sites were speculated to be responsible for the formation of such molecules as ortho and meta xylene , 1,2,4,5- tetramethyl benzene and 2,6 or 2,7 dimethylnaphtalene . However , the data as presented appear insufficient to support their proposal , because in the absence of information on diffusion

coefficients and reaction rates , one cannot rule out the effect of diffusional constaints or product selectivity . Furthermore , the surface sites are probably less active than tetrahedrally coordinated internal sites . [25]

Table 2.2 Kinetic diameters and pore dimensions of some organic molecules and zeolite respectively .

Molecule	Kinetic Diameters (Å)
CO_2	3.30
CH_4	3.80
C_2H_4	3.90
n-C_4H_{10}	4.30
i-C_4H_{10}	5.00
Benzene	5.85
Cyclohexane	6.00

Zeolite	Pore Dimensions(Å)
Chabazite	3.6 x 3.7
Erionite	3.6 X 5.2
A	4.1
ZSM-5	5.4 X 5.6 ; 5.1 X 5.5
ZSM-11	5.1 X 5.5

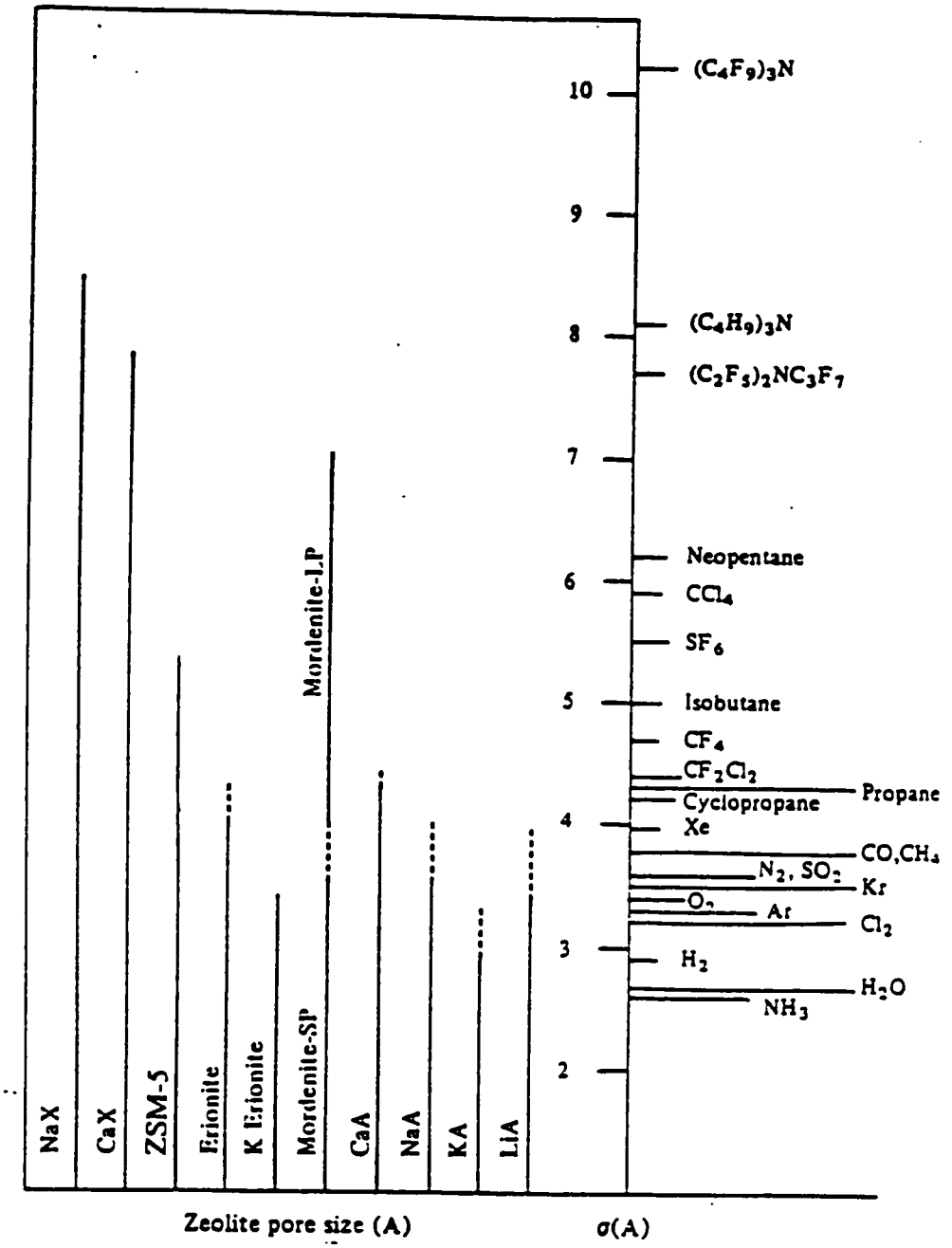

Figure 2.5 Correlation between effective pore size of various zeolites with Kinetic diameters of various molecules based on Lennard Jones Relationship .

2.2.8 Acidity of Zeolites

There are two types of acid sites which classify the active sites in heterogeneous catalysts : classical Bronsted and Lewis acid sites . According to the Lewis definition an acid is a substance that can take up an electron pair to form a covalent bond . The Bronsted-Lowry definition states that an acid is a substance that gives up a proton and the strength of an acid is dependant on its tendency to give up a proton . [26]

Catalytic activity is defined by the following characteristics :

1) the strength of acidity

2) the concentration .

3) the accessibility of the bridging hydroxyl groups which are known to act as Bronsted acid sites .[27]

Surface acid sites in zeolites are of two types :

a) Those capable of donating protons , as the bridging hydroxyl group in SiO(H)Al which is associated with tetrahedraly coordinated or framework aluminum atoms, or Bronsted acid sites (B.A.S) .

b) Those capable of accepting electron pairs from adsorbed species , like the tricoordinated Al^{3+} or Lewis acid sites (L.A.S) . [28]

These two types of sites are illustrated in fig. 2.6 . Acidity on zeolites will be therefore defined by two independant qualities : Firstly the "strength" which is defined as the ease of proton transfer from the surface sites to the adsorbed base , or of an electron pair transfer from an adsorbed base to a surface site , and secondly by the amount of acid which is given by the concentration of the respective acidic sites assuming no diffusional limitations. [29] Bronsted acid strength depends on the electronic charge of those protons associated with the bridging hydroxyl groups of SiO(H)Al in zeolite frameworks .

Each tetrahedrally coordinated Al atom contributes to one potential Bronsted acid site but since the distribution of aluminum is not uniform there exists a wide distribution of proton strength in zeolites . [30]

Therefore there are strong , medium strenght and weak acidic sites on the H-ZSM-5 zeolite . The concentration of strong acidic sites depends on the concentration of framework aluminum . An increase in calcination temperature (>500 °C) of the zeolite leads to dehydroxylation , resulting in a decrease in Bronsted acidity and an increase in Lewis acidity . Steaming results in a decrease in the concentration of strongly acidic OH groups . [31]

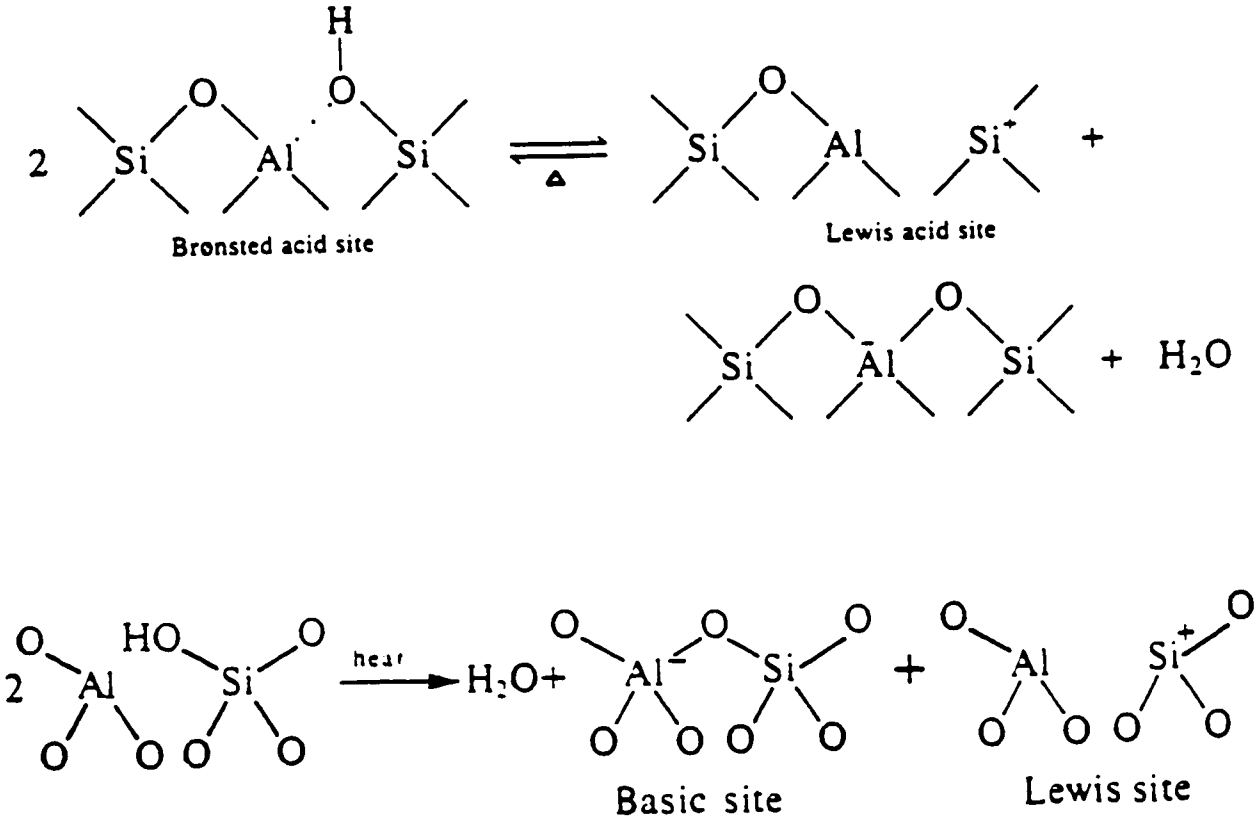

Figure 2.6 Conversion of Bronsted acid site into Lewis Center .

According to Lowenstein's rule [24] for the distribution of aluminum in the tetrahedra of zeolites aluminosilicates there are no near neighbouring AlO_4^- tetrahedra in zeolites . They are always interspersed with SiO_4 to form an electronically stable structure . Zeolites with higher Si/Al ratios or low densities of proton donor sites have high proton donor strength . [32] Because of the low concentration and specific nature of acidic sites it is difficult to accurately measure their acid strength and concentration by conventional methods such as ammonia temperature desorption and I.R spectroscopy .[33]

Doremieux-Morin et al.[34] proposed a scale for measuring the proton acidic strength of solid acids based on a calculated ionization coefficient obtained from simulated broad-line NMR spectra .Bronsted acid sites are able to ionize water molecules to form hydronium ions (H_3O^+) which can be quantified. Different concentrations of water are adsorbed onto anhydrous zeolite under vaccum and the degree of ionization of water to form hydronium ions is directly proportional to the number of acidic sites present . [34] Figure 2.9 shows a typical zeolite framework surface (a) as synthesized , where H^+ is either an alkali cation or an organic cation , (b) using the ammonium ion exchange procedure , this produces the ammonium form , (c) thermal treatment (450 °C) is used to remove ammonia producing the acidic form H^+ (d) .The acid form in (c) is in thermal equilibrium with the form shown in (d) , where there is a silanol group adjacent to a tricoordinated aluminum .

2.2.9 Manipulation of Si/Al ratio

Zeolites are grouped into families on the basis of composition , namely , the Si/Al ratio . It is known that there is a direct relationship between the chemical composition and the structural stability and purity , and also the acid strength of the bridging hydroxyls of zeolites , in particular for ZSM-5 zeolite that is synthesized . There have been three concepts which were proposed for defining the lower threshold limit in the Si/Al ratios for different zeolites . Lowenstein came up with the avoidance principle , which he proposed in the 1950's which states that whenever two aluminum atoms are neighbors to the same oxygen anion , at least one of them must have a coordination number larger than four , that is five or most likely six . [35] This applies specifically for the A zeolite (Si/Al=1) which was the only zeolite synthesized at that time , thus according to this theory , it was impossible to synthesize a zeolite with a Si/Al < 1 since all the framework Al of such a zeolite must have a coordination number of four . This rule explains the maximum substitution of 50% of the silicon in a three dimensional framework network of tetrahedra by aluminum . [36]

During the 1960's , it was proposed by Goldsmith that the crystallization of zeolites is consistent with the " simplexity principle" , which

related the ease of crystallization to structural "simplexity" . [37,38] High structural simplexity is a situation synonymous with high entropy (disorder of a metastable state) and structural simplicity for the primary building blocks (SiO_4 and AlO_4^- tetrahedra) . The growth of zeolites requires the formation of a nucleus . In a system with a high disorder , the principle favors the formation of a smaller nucleus with the highest simplexity , which may be the nucleus of a crystal in a metastable state . In zeolites , silicon atoms always exist in four fold coordination . Thus the zeolite aluminium atoms which are isomorphous substituents of Si , must assume a four coordination with oxygen so that these structures might have a higher case of crystallization (high simplicity) . We could make the contrast with other aluminosilicates as for example kaolinite and bentonite clays in which the aluminium ions are either located in four fold coordination or six fold coordination with oxygen throughout the structure . These structures are synthesized as thermodynamically stable phases . [36]

One of the most recent concepts for the determination of acidic strength of zeolites takes into consideration the nature of the cation occupying the first as well as the second shell of tetrahedra around a Si atom (secondary building blocks : SBU) and this is related to the topological densities of AlO_4^-

tetrahedra . Barthomeuf proposed that the ZSM-5 zeolite cannot be synthesized with a Si/Al ratio lower than 9.5 , since firstly , the crystallinity and stability of the structure are severely reduced if there is a higher content of framework aluminum . [36] There will be the inevitable introduction of aluminum into extraframework positions during hydrothermal synthesis as octahedral or tricoordinated Al^{3+} and this reduces the purity of the zeolite . Moreover , in accordance with Lowenstein's principle , when two tetrahedra are linked by one oxygen bridge , the centre of only one of them can be occupied by aluminum ; the other centre must be occupied by silicon or some other small ion of valence four or more (Nearest Neighbor) . For the structure of faujasite , a given Al atom must have four Si atoms in the first surrounding layer (Nearest Neighbor) and 9 Al or Si atoms in the second layer (Next Nearest Neighbors or NNN) . For the X zeolite , all of these NNN will be Al, by Lowenstein's rule . With increasing Si/Al ratio , some of the Al will be replaced with Si but at a sufficiently large ratio , all 9 NNN will be replaced with Si and the original Al site will be isolated . The strength of this Al site will depend on the number of NNN Al and will be maximum for 0 NNN Al . According to the model proposed by Barthomeuf using topological densities to include the effects of layers one through five surrounding the Al atom , the

threshold value for the limit to the Si/Al ratio for a highly crystalline ZSM-5 is 9.5 . [36]

2.2.10 Adsorption in Zeolites

The void spaces in the crystalline structures of zeolites provide a high capacity for adsorbates , referred to as guest molecules . The sorption capacity is a conveniently measured property that is used to identify zeolites .[39]

The usual steps for transport phenomena during heterogeneous catalytic activity involves the following sequence :

1) Diffusion of gaseous reactant molecules from the bulk phase to the gas/solid interface .

2) Diffusion into the catalyst pores .

3) Adsorption

4) Reaction at the active sites .

5) Desorption of the product molecules away from the latter .

6) Counter diffusion of product molecules through the catalyst pores .

7) Counter diffusion to the bulk phase .

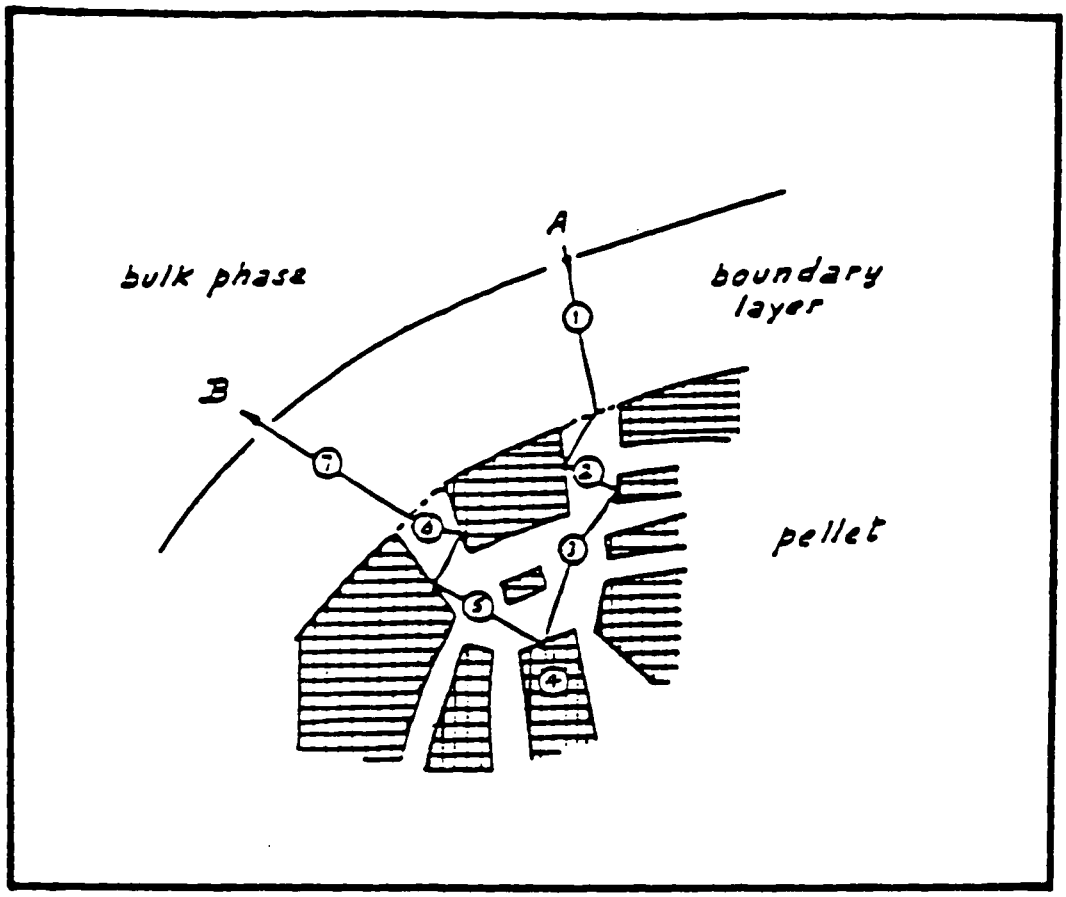

Figure 2.7 Transport Phenomena of Heterogenous Catalysis : Physical and Chemical steps .

In most cases steps 2) , 3) and 4) are usually not distinctly resolved and ideally steps 1) and 4) should be very fast for reactions that are not diffusion limited . [39]

2.2.11 ZSM-5 Zeolite and Silicalite

The group of solids having the composition SiO_2 , will be expanded by replacement of some of the Si atoms with Al . The compound SiO_2 is stable in the gas phase , having a structure with two Si=O bonds resembling that of CO_2 . There is a large free-energy driving force for the self-association of the SiO_2 molecules , with conversion of the Si=O bonds into Si-O bonds . Many geometries of the resulting condensed structures exist , two of the best known being quartz and cristobalite , and another being silicalite , which is closely related to a zeolite . All of these are crystalline , with each Si atom in tetrahedral surroundings , sharing bridging oxygen atoms with neighboring Si atoms . Silica being a non-crystalline material has the composition SiO_2 .

The SiO_4 tetrahedra can be combined in many arrays with the sharing of oxygen atoms . When they are arranged , the result is the secondary building block of silicalite . When some Si atoms in this structure are replaced by Al atoms , the resulting aluminosilicate is referred to as ZSM-5 , a zeolite

and an industrially important catalyst . [40]

The ZSM-5 zeolite exhibits a two dimensional network of channels having a structure as illustrated in fig. 2.10 . There exists two distinctive pore types intersecting each other and both are formed by 10 membered oxygen rings .One pore type varies from 5.1 x 5.5 Å in straight but ellipsoidal rings , the other zig-zags and has circular openings of 5.4 x 5.6 Å . In thus possesses a mean average pore diameter of 5.5 Å with a Si/Al ratio ranging between 10 and 500 .Because of its pore structure it exhibits a high degree of shape selective catalysis and has many useful applications in petroleum refining particularly in enhancing gasoline octane when this zeolite is used as a catalyst additive in gas oil cracking .

Many properties of ZSM-5 such as its ion-exchange capacity and hydrophobicity are dependent on its chemical composition (Si/Al ratio) . Its attractiveness as a catalyst is due to its intrinsic acidity arising from its low aluminum content which can be varied over a large range of concentrations giving rise to catalytic activities that can be predictably changed over many orders of magnitude . According to Olson et al.[41] , the ion-exchange capacity and catalytic activity increases with the aluminum content .

In fig. 2.8 (Variation of acidic strength (hexane cracking) with

aluminum content of zeolite) , we see that there is a linear relationship between n-hexane cracking activity and the aluminum content . On the other hand the hydrophobicity increases with the decreasing aluminum content. [42]

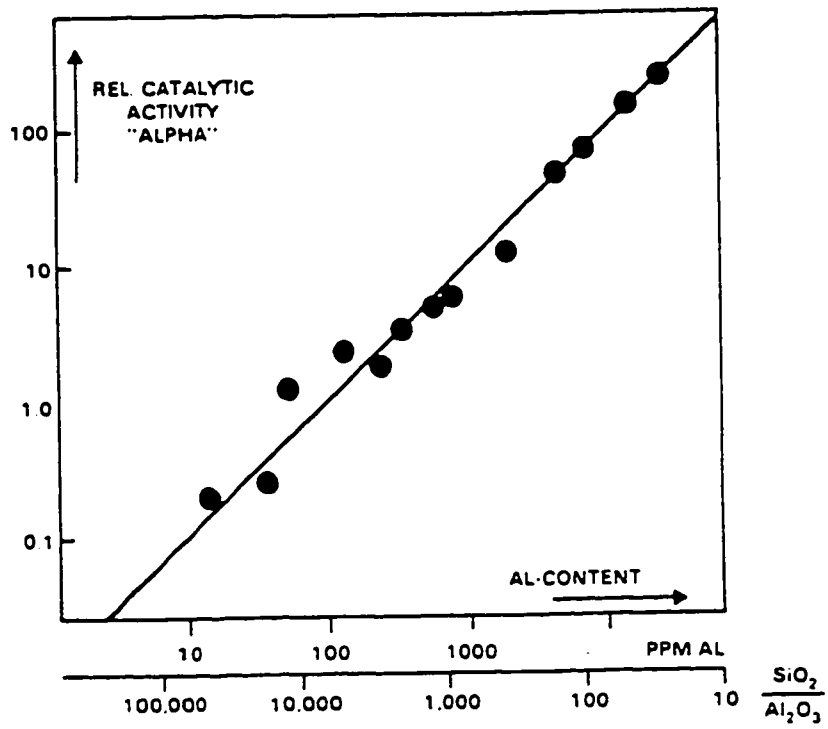

Figure 2.8 Variation of acidic strength (Hexane Cracking) with aluminum content of zeolite .

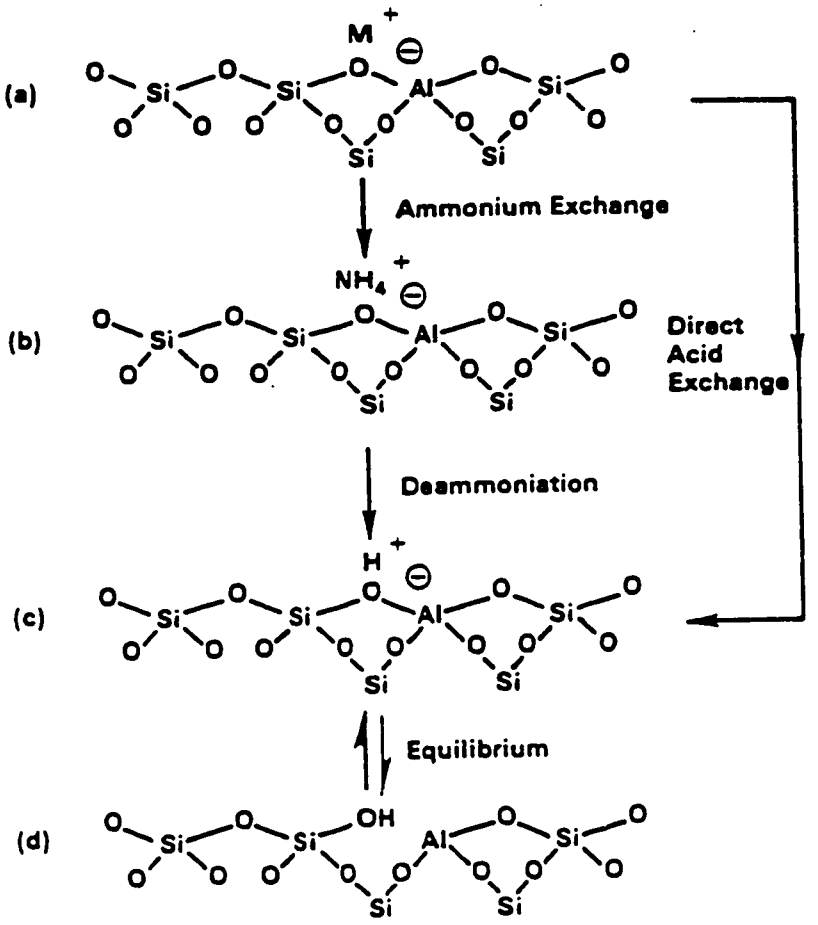

Figure 2.9 Typical Zeolite framework surface a) as synthesized , M^+ is either an alkali cation or organic cation , b) Ammonium ion exchange procedures produce the NH_4^+ form , c) thermal treatment (450 ^{0}C) is used to remove ammonia producing the H+ acidic form , d) the acid form in c) is in thermal equilibrium with the form in d) and we find a silanol group adjacent to a tricoordinate aluminum .

According to Barthomeuf et al. a lowering of the Si/Al ratio is congruent with an increase in the number of acid sites but the acidic strength of bridging hydroxyls in SiO(H)Al species increases as the Al content decreases because of the isolated nature of the latter in these zeolites . It has been found by Barthomeuf et al. using experimental data on the topological densities of isolated AlO_4 tetrahedra in zeolites that the limiting Si/Al ratio for preparing the ZSM-5 is 9.5 [43,44] . Some of the benefits which are associated with a high Si/Al catalyst are : oil refining , organic synthesis and include superior efficiency , easier seperations and handling as well as greater stability and environmental factors (see table 2.3).

Table 2.3 Large Scale Processes Catalyzed by ZSM-5

Petroleum:	
Catalytic Cracking	Distillate Dewaxing
Light Paraffins to Aromatics	Refining
Synthetic Fuels and Chemicals:	
Methanol to Gasoline	Olefins to Gasoline and Distillate
Dehydration of Ethanol	
Chemicals :	
Xylene Isomerization	Toluene Disproportionation

Another very important commercial application of these zeolites is as ion-exchangers , they are comparable to the sulfonated resins . If we bring an aqueous salt solution in contact with the zeolite this would lead to the incorporation of cations from the salt into the zeolite , replacing some of the non-framework cations initially present . Ion-exchange is the simplest and one of the most important methods for modifying the properties of a zeolite .

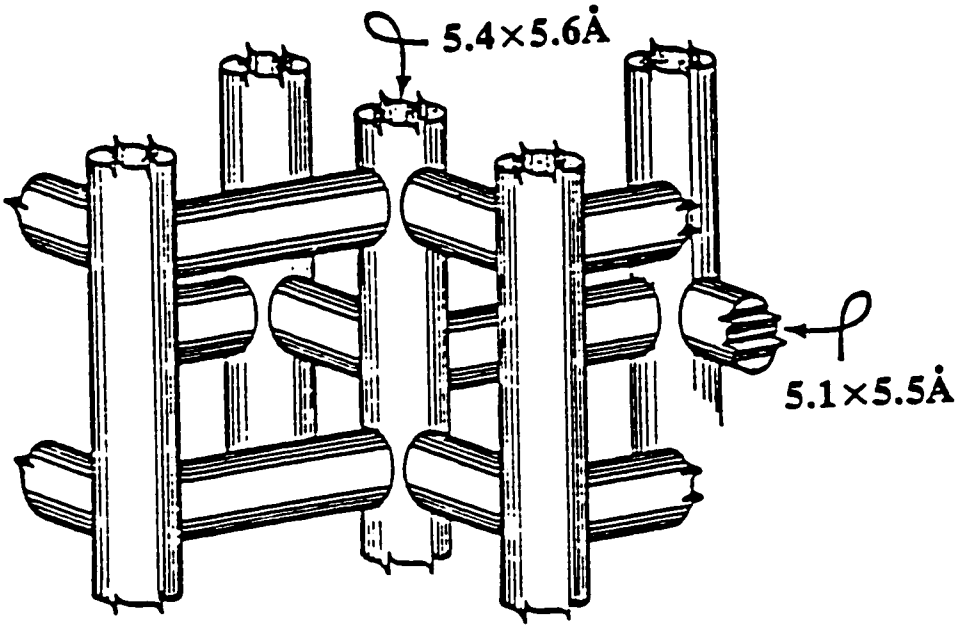

Figure 2.10 Structure of ZSM-5 Zeolite

2.2.12 Faujasites (X and Y zeolites)

The faujasite - type zeolites X and Y have a network of three - dimensional intersecting channels in which the minimum free diameter is the same in each direction . Zeolites X and Y have a Si/Al ratio of about 1.3 and 2.5 respectively . These zeolites are isostructural with naturally occuring faujasites , and consist of an array of cavities having internal diameters of about 12 Å . The access to each cavity, which is also termed supercage is through six equispaced necks having a diameter of about 7.4 Å formed by a ring comprising 12 oxygen atoms . X and Y zeolites have among the largest minimum aperture restrictions of any zeolite , and the highest void fraction . The faujasite structure may be seen in fig. 2.11 . [45]

Synthetic X and Y zeolites are used almost exclusively as commercial cracking catalysts . The catalytic properties of these materials are related to the aluminum framework content which affects the magnitude of the cubic unit-cell parameter a [46] .

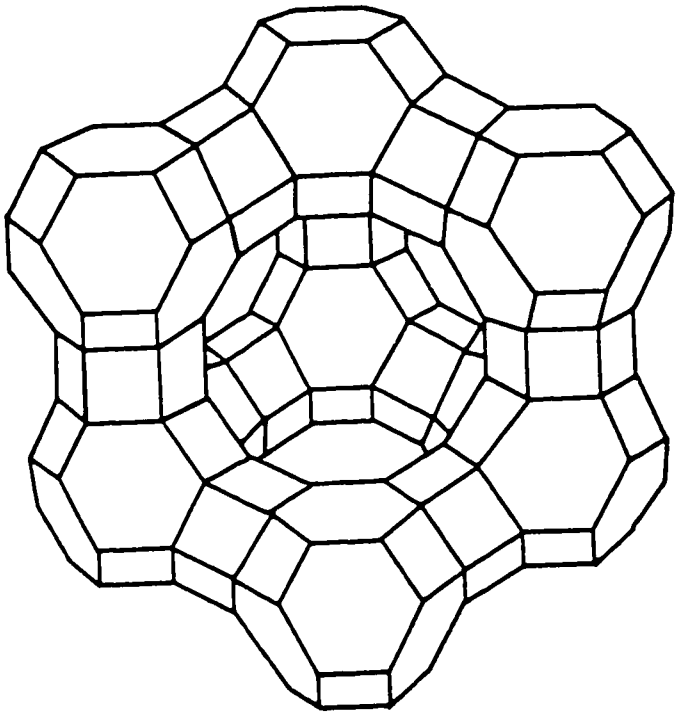

Figure 2.11 Typical Faujasite Structure .

Chapter 3

Experimental

3.1 Source of Materials

Chemicals	Supplier
Na-X	Linde Molecular Sieves
Na-Y	Linde Molecular Sieves
Na-ZSM-5	Chemie Uetikon AG
NH_4-ZSM-5	Zeolyst International
Silicalite	UOP Molecular Sieves
Hydrogen Chloride (12M)	BDH
Sulfuric acid (18M)	BDH
Lithium Tetraborate	Aldrich Chemicals inc.
Potassium Carbonate	Aldrich Chemicals inc.
Sodium Carbonate	ACP Chemicals inc.
Sodium Hydroxide (19.4N)	Aldrich Chemicals inc.
Ammonium Chloride	ACP Chemicals inc.
(Si-O) species	In our Laboratory
KBr (FT-IR) grade	Aldrich Chemicals inc.
Sodium standard (1000ppm)	Fisher Scientific
Aluminum standard (1000ppm)	Fisher Scientific
Hydrogen Peroxide (30%)	ACP Chemicals inc.

3.2 Introduction

This chapter describes the development and optimization of the desilication procedure and the characterization of the desilicated materials. The process for the silicon removal has been developed as a way to generate materials which have an improved catalytic activity due to a higher density of proton sites . We could define desilication as a selective removal of silicon from highly siliceous materials using a mildly alkaline solution . This has the effect to decrease the Si/Al ratio in a systematic manner and is a direct means of increasing the cation exchange capacity of the solids [47] .

The desilication of commercially available silicalite , Na-X , Na-Y and Na-ZSM-5 zeolites is studied for the effect on their textural and chemical properties .This new treatment of desilication using an aqueous solution of sodium carbonate and optimum conditions will be described . The desilicated materials have also been shown to be very good in non-catalytic applications for the removal of calcium and magnesium ions due to their potential of being detergent builders .

Another important application is shape selectivity . By performing the desilication on the ZSM-5 , we want to see the change in the pore size from its starting point which is for the non-treated zeolite (Parent) .

3.3 Treatments

3.3.1 Desilication

The application of a strongly alkaline solution medium on the one hand represents the conditions for the zeolite synthesis , but on the other hand silicates can be dissolved in an alkaline solution [48] . The removal of silicon atoms from highly siliceous zeolites using hot alkaline solutions of either sodium carbonate, which hydrolyzes to sodium hydroxide, or the sodium hydroxide directly, results in severe structural collapse [49,50] . In addition there is the possibility of other species recrystallizing from the solution especially during the treatment of zeolites with high aluminum content [51] .

Recently LeVan Mao et al.[23] developed a technique whereby silicalite and other silica rich zeolites such as the Na-ZSM-5 , and lower Si/Al ratio zeolites such as Na-X and Na-Y zeolites , were treated with mildly alkaline solutions of sodium carbonate in such a way to effect the selective removal of silicon atoms from these structures [50] .

3.3.2 Experimental

3.3.2.1 Sample Preparation

The Na- ZSM-5 zeolite was purchased form Chemie Uetikon AG , the NH_4- ZSM-5 zeolite was purchased from Zeolyst International , and both the Na-X and Na-Y were purchased form Linde Molecular Sieves . All of these were in powder form and activated at 120 ^{0}C prior to treatment .

3.3.2.2 Desilication

A) Na-ZSM-5 and NH_4-ZSM-5

Both forms of ZSM-5 were treated with a basic solution of 0.8M sodium carbonate and 0.01N of sodium hydroxide which has a pH measured to be 11.3 (1g of zeolite/30ml of solution) for a period of 4 hours at 80 ^{0}C with mild stirring (60 RPM) .The mixture was allowed to settle and the supernatant decanted while fresh solution was added . The treatment was repeated 3 times until the total time of treatment of the material was 12 hours . The resulting desilicated material was washed with (1-2) liters of warm water to complete the removal of silica and sodium silicate and then the material was dried at 120 ^{0}C. These are hereafter referred to as NaDZSM-5 (1) for the desilicated Na-ZSM-5 , NaDZSM-5 (2) for the desilicated NH_4-ZSM-5 . These samples were characterized by atomic absorption

(chemical composition) , X-ray diffraction for crystallinity, and BET measurements for textural properties of surface area and pore size distributions as well as by ^{29}Si and ^{27}Al NMR for the configuration of aluminum in the zeolite framework for both the parent and desilicated zeolites (all data reported in the results section) .

B) Na-X and Na-Y

Both of these samples were activated at 120 ^{0}C and then they were treated with sodium hydroxide in different ways . Na-X was treated with sodium hydroxide in a range of 0.2N to 0.4N and the Na-Y in a range of 0.1N to 0.3N . The samples were then washed with some warm distilled water and dried at 120 ^{0}C. From the characterization results the optimal concentration of sodium hydroxide was determined for each zeolite .

3.3.3 Extraction of the (Si-O) species

The orthosilicate species could not be purchased from any supplier . It was therefore extracted from the desilication washing waters . By combining all of these solutions , and evaporating the aqueous phase, a white solid is obtained which is then dried in the oven at 120 ^{0}C for a few

hours .The solid was found to contain orthosilicate and pyrosilicate in majority and trace amounts of other species .

3.3.4 Impregnation using the (Si-O) species

We prepared samples with different amounts of orthosilicate going from 1% weight to 5% weight . For a sample of 2.5% weight , 5 g of desilicated zeolite were mixed with 0.125 g of orthosilicate . The Si-O species was first dissolved in 50 ml of water and heated to 80 ^{0}C for 2 hours . Then the 5 g of desilicated zeolite was mixed with the dissolved (Si-O) species and heated for another 2 hours at 80 ^{0}C until dryness . The sample was then heated in the oven to 120 ^{0}C overnight to remove any water.

3.4 Thermal Treatment

Desilicated and non-desilicated samples are said to be activated at high temperatures, have been specifically heated in air for periods of 12 to 16 hours . The activation temperature varied between 350 ^{0}C to 700 ^{0}C, all depending on the sample analyzed .

3.5 Steam Treatment

This type of treatment uses a lower temperature than thermal treatment , which is usually in the area of 300 ^{0}C . The amount of water used for the steam treatment is approximatively 13 ml for a period of 2 hours . The flow rate was measured to be 6.19 ml/h . A flow of nitrogen is passed through the sample for a period of 30 minutes at the end of the steaming process to remove the water that might remain .

3.6 Calcium and Magnesium ion-exchange Testing

The selectivity for the removal of calcium and magnesium was studied by ion-exchange capacity testing. The initial rates of ion exchange for the zeolite samples Na-X and Na-Y varied with the variation in temperature from 25 to 60 ^{0}C . The investigation was done on the ion-exchange capacities of the desilicated X and Y zeolite (prepared as mentioned in part 3.3.2.2b) .

The ion-exchange testing was performed for a solution made out of calcium chloride and magnesium sulphate . The experimental set up was designed to simulate the actual working conditions for detergent powders in washing machines. A volume of 500 ml of hard water was placed in a flask

containing a stirring bar . This flask was then set up a top of a stirring hot plate which achieved a strong and constant stirring action throughout the experiment .It was very important to have homogeneity in the exchange media , this was a key factor for data reproducibility . At the specific temperature of the solution , 1 g of the zeolite sample was poured into the flask and aliquots were taken at intervals of 3 minutes for a period of 30 minutes. C_i Ca is the initial concentration of calcium ions removed and C_fCa the final concentrations of calcium ions removed, both expressed in ppm. . The value of C_i Ca was calculated by replacing "t" by zero in the Rca equation below. C_f Ca was calculated by replacing "t" in the Rca equation by 30 minutes . Magnesium ion removal (IR Mg) was determined in the same manner as the calcium ion removal . The total ion removal was expressed as :

$$\text{IR tot (equiv.based \%)} = [1-(C_f\,Ca + C_f\,Mg) / (C_i\,Ca + C_i\,Mg)] \times 100$$

The rate of calcium ion (or magnesium ion) removal (ppm/min) is given by the following equation :

$$Rca = dy/dt = b + 2ct$$

The initial rate of calcium removal was determined by taking t = 0.

Thus : [Rca] = b (ppm/min)

The rates of removal were calculated in the same way for the calcium and magnesium ions .

3.7 Physico-Chemical Characterization techniques

The main techniques which were used in this project to characterize the samples included : BET measurements , Atomic absorption Spectrophotometry, X-ray powder diffraction and MAS - solid state NMR (^{29}Si and ^{27}Al) .

3.7.1 BET Specific Surface Area

The most useful method to determine the total surface area of a solid material which requires non-specific physical adsorption , is called the BET method for Brunauer , Emmett and Teller . The surface area , which is a very important textural parameter of a solid , can be used to define the morphology and surface characteristics . The specific surface area (A) is the measure of the accessible surface area per unit mass of solid , where this surface is the sum of the internal surface area associated with pores and of the

external surface area developed by the outer boundary of the particles [51,52].

The determination of A includes the following steps :

1) Setting up the adsorption isotherm by measuring the volume of nitrogen adsorbed versus the relative pressure of the adsorbate ,

2) Evaluating the monolayer capacity (V_m) from the isotherm ,

3) Converting V_m into A by means of the molecular area (A_m) .

The theory of BET is based on a kinetic model of the adsorption developed by Langmuir [51] in which the surface of the solid is regarded as an array of adsorption sites .The BET theory is based on the following three assumptions :

A) There is no interaction between molecules adsorbed in the first layer of a homogeneous surface with equivalent sites for localized adsorption .

B) Each molecule in the first layer is a possible site for adsorption of a molecule in the second layer , and so on in order to get a multilayer adsorption .

C) With the exception of the first layer , the heat of adsorption is equal to the molar heat of condensation and the evaporation-condensation conditions are identical in all others .

The physical and mathematical treatment of these hypotheses leads to the following BET equation :

$$P / V(P_0-P) = (C-1)\, P/V_mCP_0 + 1/V_mC \qquad (1)$$

Where : P = is the equilibrium pressure of the adsorbate .

P_0 = Saturated vapor pressure of the adsorbate in the condensed state .

V = Volume of the gas adsorbed at Standard temperature and pressure .

V_m = Volume of gas at STP corresponding to the formation of a monolayer coverage .

C = A constant varying with the adsorbent - adsorbate interactions which is related to the differential heat of adsorption E_a, and to the heat of liquefaction E_L, by the following relation :

$$C = \text{Exp.}\ (E_A - E_L) / RT$$

Where : R= Ideal gas Constant

T = Absolute Temperature

The graph of $P / V(P_0-P)$ versus P/P_0 at a pressure range of ($0.05<P/P_0<0.35$) should give a straight line hence ,from which one should be able to derive C and V_m . As mentioned previously , the BET method for calculation of a specific surface area (A) involves two additional steps :

A) Evaluation of the monolayer capacity (V_m) from the isotherm . To obtain a reliable value of V_m from the isotherm , it is necessary that the monolayer be virtually complete before the build up of additional layers starts : which is met if the BET parameter C is neither too low nor too high

B) Conversion of V_m into A by means of the molecular area (A_m) . Since nitrogen comes the closest to meeting these conditions when adsorbed on an extensive range of solids , it has become the most generally used adsorbate for surface area determination . The specific surface area of the adsorbent is then given by : $A = A_m (V_m N) / V$ (3)

Where : N = Avogadro's Number

A_m = Area occupied by one molecule of adsorbate Am (N_2) of 16.2 $Å^2$ is the widely accepted value [52] .

3.7.2 Pore Size Distribution Measurement

The pore size distribution is defined as the distribution of the specific area versus the pore size . It is an important textural parameter for the determination of morphology and pore structure of a porous solid . Depending on the pore size range of a solid , the appropriate technique is applied . [52]

Techniques based on nitrogen adsorption/desorption isotherms make use of the desorption loop of an adsorption isotherm to relate the amount of adsorbate lost in a theoretical desorption step to the average size of a the pore emptied during the step . A pore loses its condensed liquid adsorbate at a pressure related to the pore radius by the Kelvin equation on the assumption of cylindrical pores when the adsorbate surface tension , contact angle, and molar volume are known for the adsorption temperature . However , even when a pore has been emptied of condensed liquid , multi-layers of adsorbed molecules remain on the inner surface of the pores and these multi-layers continue to thin down as desorption proceeds . Therefore , the measured desorption is made up from the removal of condensed liquid from some pores , plus the adsorbate lost from the surfaces exposed in earlier steps .

The classical method consists of adsorption of N_2 at saturation under liquid nitrogen and then by applying vacuum , the adsorbate is generally

removed . When $P/P_0 \rightarrow 1$, where P_0 is the saturation pressure , all the pores are completely filled with adsorbed and condensed nitrogen . When the pressure is lowered by small increments , a small amount of nitrogen will first evaporate from the meniscus formed at the ends of the larger pores . Hence , a desorption isotherm of volume desorbed versus pore radius is established . The pore size distribution of a mesoporous solid may be calculated from the desorption isotherm of a vapor with the help of the Kelvin equation :

$$\ln P/P_0 = -2\, nV/RT \times 1/r_K \cos\theta \qquad (4)$$

Where : P/P_0 is the relative pressure of vapor in equilibrium with a meniscus having a radius of curvature r_K .

n is the surface tension of liquid adsorbate .

V is the molar volume of liquid adsorbate

R is the ideal gas constant

T is the absolute temperature

θ is the contact angle between the capillary condensate and the adsorbed film on the walls .

The concept of capillary condensation and its quantitative expression in the Kelvin equation is the basis of virtually all the various procedures for the

calculation of pore distribution . When capillary condensation occurs during the course of the isotherm determination , the pore walls are already covered with an adsorbed film , having a certain thickness (t) determined by the value of the relative pressure . Capillary condensation therefore , does not occur directly in the pore itself but rather in the inner core (fig. 3.1) .

The conversion of an r_K value to a pore size requires recourse to a model of shape and a knowledge of the angle of contact θ (it is assumed that $\theta = 0$ hence $\cos \theta = 1$) . Several methods which make use of Kelvin's equation and attempts to correct the Kelvin radius , have been proposed . However , all these computational methods can give an accurate assessment and measurement of the macro- and mesopores but not the micropores .

Pore size distributions can be computed using a simplified model proposed by Pierce [53] , based on the application of Kelvin's equation to nitrogen desorption isotherms , from which the following is proposed :

1) All pores have cylindrical geometry .

2) The Kelvin equation is applicable for computing the pore radii from the relative pressures at which desorption occurs .

3) The film thickness remaining on pore walls after the inner capillary volume is desorbed in the same manner as on a non-porous surface at the

same relative pressure (area of the core walls is identical to the area of the pore walls , as desorption progresses) . By summing the values of pore area, (γA_P) , for each successive group of pores over the whole pore system , a value of cumulative surface area $S_{cum} = \Sigma \gamma A_P$ is obtained [53] . And this cumulative surface area reports the total area of macro- and mesopores and excludes the pore area of micropores since the validity of Pierce's method only extends down to a pore radius of 15 Å .

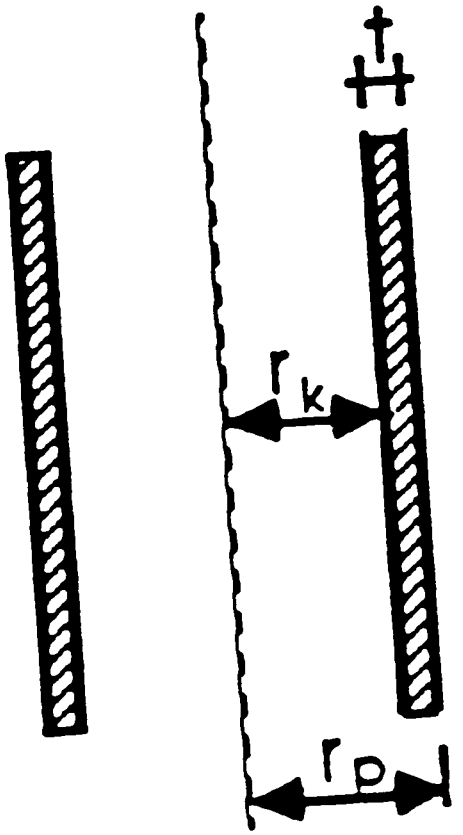

Figure 3.1 Cross Section Along the Pore Axis

3.7.3 Measurement For Micropores

Macroporous materials have pore sizes greater than 500 Å , whereas mesoporous ones have pore sizes within the range of 20-500 Å .It is to be noted that the BET surface area can be obtained without limitations . However in the presence of large quantities of micropores (pore sizes < 20 Å) such as the ones we find in the ZSM-5 zeolite , it becomes more practical to apply the Langmuir isotherm for estimating the Langmuir surface area . Since the size of the adsorbate molecules is of the same order as the pore sizes , a free multilayer adsorption such as what occurs in the BET theory does not occur without perturbation by interactions between the walls of the zeolite . Because the Langmuir treatment gives a more practical assessment of surface area , the Langmuir surface area has also been reported .

The micropore size distribution was determined by the adsorption of argon at 87K using the Micrometrics model ASAP 2000m and the data interpretation model by Horvath Kawazoe [52] .

3.7.4 Instrument Used

The ASAP 2000 system , as shown in figures 3.2 and 3.3 , is used for macro and meso pores analysis and it consists of either one or two analyzers and a multi-function control module . The separate internal vacuum systems are included in the analyzer : one port for sample analysis and two ports for sample preparation . Between the vacuum pump and the manifold in both the degassing and the analysis system , are located the in-line cold traps . The sample saturation pressure (P_0) tube is located next to the sample analysis port beneath which is conveniently located the automatically operated elevator with the liquid nitrogen (LN_2) Dewar mount . Connectors are put near each sample preparation port for the mounting of heating mantles and thermocouples . Controls and indicators on a swing-open control panel can provide operation of the vacuum system , degas valves and heating mantles for sample preparation . The control module consists of a computer equipped with the ASAP 2000 software .

The ASAP 2000m looks very similar to the ASAP 2000 , but the only difference lies in the fact that at the analysis port , the dewar mount is filled with argon instead of N_2 . The other obvious difference is that we have adsorption of argon instead of nitrogen .

The micropore size and distribution of the desilicated zeolites used for the optimization of the desilication procedure [48] , and all other zeolite samples studied by this technique thereafter in this thesis , were calculated using more suitable values of the interaction parameter (IP) . These new values gave more accurate results than the empirical values to obtain the average values of the micropore sizes in the first samples studied by this technique [49] .

Moreover for the measurements of the BET and Langmuir surface area and for micropore size determination , an outgassing temperature of 150 ^{0}C was used in order not to favor any advanced healing process which was observed to occur at high temperatures of activation [59] .

The interaction parameter, as recommended by Horvath Kowazoe was 5.89 x 10^{-43} ergs/cm^4 for microporous solids [59] and by Micrometrics Corporation for zeolites was 3.19 x 10^{-43} ergs/cm^4 [60] . We found that for the ZSM-5 zeolites the best value for the IP was found to be 4.9 x 10^{-43} ergs/cm^4 for the Y zeolite 4.6 x 10^{-43} ergs/cm^4 and for the X zeolite 5.2 x 10^{-43} ergs/cm^4 .

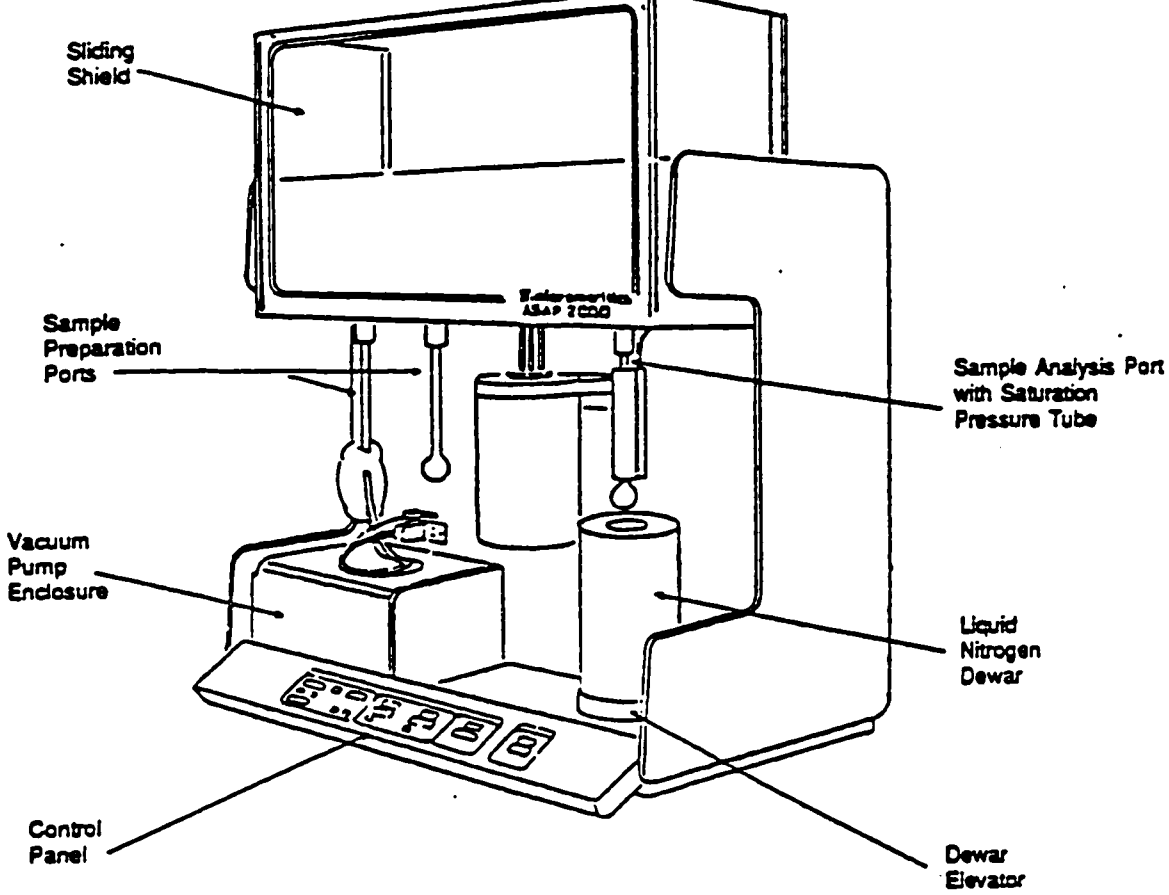

Figure 3.2 ASAP 2000 System

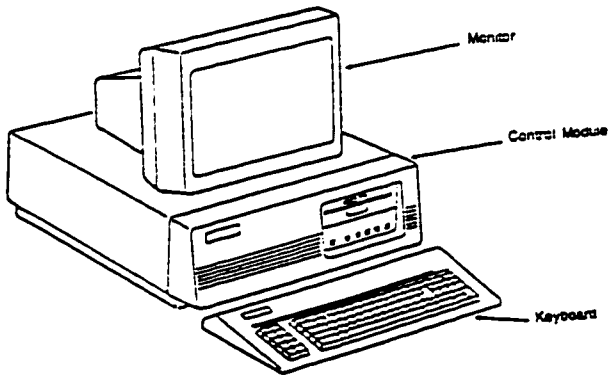

Figure 3.3 The Control Module

3.7.5 Procedure For Sample Preparation

The samples were heated at 120 ^{0}C in air overnight before performing the BET (N_2) or micropore (Ar) analysis . A clean BET tube was degassed down to less than 10 μm Hg pressure . Then the tube was weighed out empty , the sample was then evacuated while heating it at 220 ^{0}C for 4 hours in the case of nitrogen analysis and for at least 12 hours in the case of argon analysis . After cooling the tube down to room temperature , the weight was recorded and it was inserted with other data in the ASAP 2000 program . The analysis was performed in about 4 hours for the nitrogen analysis and 24 hours for the argon analysis of the ZSM-5 , Na-X and Na-Y . These instruments give the results within a range of $\pm$ 7% [60] .

3.8 Atomic Absorption Spectrophotometry

3.8.1 Procedure for chemical analysis

The method used for analysis of our zeolites consisted in weighing out accurately 0.12g of our zeolite sample in a platinum crucible . This crucible was then placed in an oven at 800 ^{0}C for a period of 2 hours . It was then cooled and reweighed to obtain the dry weight . 0.9g of fusion mixture (potassium carbonate and lithium tetraborate in a ratio of 2:1) was added to the zeolite material , mixed and ashed in the furnace for another 2 hours at 800 ^{0}C , this helps complete the decomposition of the zeolite . The resulting mixture was transferred to a 150 ml beaker and digested with a strong mineral acid mixture of 4 ml of Hcl (12M) and 10 ml of H_2SO_4 (10%) solution . The beaker was covered with a watch glass to avoid any sample loss . The mixture was then heated on a hot plate for 30 minutes , then 4 ml of 30 % hydrogen peroxide was added and the dissolution mixture was further digested for a few minutes until effervescence stopped . The final mixture was heated overnight on a hot plate . Then the solution was cooled and was transferred to a 100 ml volumetric flask and it was diluted to the mark with distilled water . Appropriate dilute solutions were prepared from this stock solution . The standard solutions were prepared from 1000 ± 0.2 ppm metal

made every few months to assure a good standard curve .

For the analysis of aluminum for example , five standard solutions which ranged from 10 ppm to 50 ppm were prepared . Finding the absorbance of these solutions enabled us to draw a standard curve, and from this curve we were able to find the concentration of solutions to be analyzed, knowing their absorbance .

The % of oxide present was determined using the following equation :

$$\% \text{ Element} = R_a/R_{std.}\ (C_{std.}/W_a)(V_a)(M/F)(D.F) \times 100 \quad (12)$$

where : R_a = reading obtained from the sample solution

$R_{std.}$ = reading obtained from the standard solution

$C_{std.}$ = concentration of standard solution (ppm)

W_a = weight of the dried sample (g)

V_a = volume of original sample solution used (ml)

M = molecular weight of element in the oxide form (g/mole)

F = Formula weight of element (g/mole)

D.F = dilution factor

We could define the dilution factor using the following equation :

$$D.F = Vds./ Vad.$$

where : Vds. = volume of the diluted sample solution (ml)

Vad. = volume of aliquot taken from the dilution (ml)

To determine the Si/Al ratio , we used the following equation :

$$Si/Al = 0.5 \ [(WSiO_2) / (WAl_2O_3)] \times [(MWAl_2O_3) / (MW\ SiO_2)]$$

where : W = weight percent

MW = molecular weights

3.9 X-Ray Powder Diffraction

3.9.1 Procedure

All of the samples were preheated at 550 ^{0}C overnight and left in the oven at 120 ^{0}C before the XRD analysis was performed . When a desilicated sample was analyzed on a certain day , the parent sample heated in the same manner was also analyzed on the same day . This method of analysis insured that any fluctuation in the instruments' precision, which sometimes changes from day to day, was taken into account . The samples were ground well and were placed into a plexiglass holder . Each sample was scanned in the region $5^0 < 2\theta < 60^0$ and the counts were recorded automatically at a scan speed of 0.5^0/min and a step size of 0.02^0 .The peak intensities were taken as the number of counts recorded by digital integration during a complete scan at constant angular velocity . Background correction was done by subtracting the baseline using the Sietronics software .The degree of crystallinity (DC) of the sample was determined using the following equation :

$$DC\ (\%) = I_0/I\ (100) \quad (16)$$

where : $I_0 = \Sigma$ peaks intensity for the sample .

$I = \Sigma$ peaks intensity for the external standard .

We used the established method (ASTM) , which was to choose the five most intense peaks for the XRD pattern of the ZSM-5 zeolite for analysis in the range of 2θ mentioned above . All measurements were done in duplicate and the % error on all measured values was within 5 % .

To determine the composition of our compounds , the Joint Committee for Powder Diffraction Standards (JCPDS)and the micro powder diffraction search-match of Fein Marquat (μPDSM), were used for phase identification after the samples were analyzed .

3.10 Magic Angle Spinning ^{29}Si and ^{27}Al NMR .

3.10.1 Theory

Many new techniques have been developed of to help overcome the broadening obtained when applying conventional NMR to crystalline or amorphous solids and make the acquisition of very high resolution spectra , just like for liquids, possible . The more modern NMR techniques involve magic-angle spinning and they are potentially more powerful for studying the local structure of silicates and other inorganic solids that have non-zero nuclear spin nuclides [54,61] (^{29}Si and ^{27}Al for silicas , aluminas , zeolites and various other aluminosilicates ; ^{11}B and ^{29}Si for borosilicates , etc... [54,62]) . Using MAS-NMR has some advantages when we are looking at the structural insight because it probes the immediate environment of a particular nucleus without putting any emphasis on the fact that the sample may or may not be crystalline .

Finding out the coordination of ^{29}Si MAS-NMR in zeolites has proven to be very important in light of the fact that one of the major treatments deals with silicon removal (desilication) .In the case of ^{27}Al MAS-NMR it helps us to determine if the framework aluminum has changed in any shape or form . It also supplements the information provided by ^{29}Si MAS-NMR on the

alumina-silicates [63] . Most of the line broadening that we see in the NMR of solids is attributed to 2 interactions : 1) chemical shift anisotropy and 2) static dipolar interactions , which in liquids averages to zero because of the rapid and random motion of molecules . The line broadening represented by chemical shift (shielding) anisotropy is an inhomogeneous broadening , a superposition of spectra of randomly oriented individual nuclei with respect to the relative direction of the applied magnetic field . Each of these nuclei has an inherently sharp line for a particular orientation of nuclear environment with respect to the static field . When we have immobile species such as powdered crystalline solids , the net result of the chemical shift anisotropy is that the entire range of chemical shift spanned by all possible orientation is present in the spectrum . MAS-NMR is a technique that will remove the chemical shift anisotropy by a high - speed mechanical motion of the rigid sample about an axis making an angle of 54.7^{0} , called "magic angle" , to the direction of the static magnetic field [54,64,65] . In effect , the solid acts like a liquid when spun at that magic angle .This value was found by taking the time-independent parts of the transformed secular Hamiltonians which are reduced by the factor $\frac{1}{2}(3\cos^2\theta - 1)$ which vanishes for the magic angle $\theta = \arccos 3^{-1/2} \approx 54.73^{0}$. In practice , anisotropic and static effects in a solid

average out to simulate the situation present in a liquid when rotated at that magic angle .

3.10.2 Instrument Used

The MAS-NMR spectra of the zeolite materials were obtained using a Bruker ASX-200 spectrometer operating at 39.76 MHZ with a spinning rate of 4Hz . All of the ^{29}Si MAS-NMR spectra were referenced to tetramethylsilane (TMS) at 0 ppm and for the ^{27}Al ,we used $Al(H_2O)_6^{3+}$as reference . The MAS-NMR spectra were recorded at the University of Ottawa .

3.11 Fourier Transform (FTIR)

3.11.1 Application to Zeolites

Fourier transform infra red spectroscopy (FTIR) was used to detect any change in the aluminum environment , density change brought about by desilication . We also used this technique to determine if there was any structural change of the zeolite sample .

3.11.2 Instrument

The instrument used was a Nicolet Magna I.R using a Fourier transform infrared . The region of 400-1400 cm^{-1} was scanned in the transmission mode with a resolution of 2 cm^{-1} .

3.11.3 Procedure

All samples were heated at 550 ^0C overnight . The next step was to make a mixture of (1.5-2.0)% of zeolite in KBr . The amounts used were in the region of 0.0129g for the zeolite and 0.8024g for the KBr .A mortar and a pestle were used to prepare a homogeneous mixture . The resulting sample was put in the oven at 120 ^0C for a few hours until it was ready to be used , this avoided any great amount of humidity absorption by the sample .

3.12 Experimental Uncertainty

3.12.1 Desilication

The experimental uncertainty for the desilication procedure on the very important Si/Al ratio was calculated as follows .

Example : NaDZSM-5 (1)

Trials for the Si/Al Ratio : 1) 16.5 2) 17.0 3) 16.0

Average of : 16.5

Standard Deviation = $(\sum (x_i - x_{avg.})^2 / n-1)^{0.5} = 0.5$

Experimental Uncertainty = $\pm$ ts / $(n)^{0.5} = 4.3\ (0.5) / 2^{0.5} = \pm 1.2$

So the uncertainty value is : 16.5 $\pm$ 1.2 .

where : the parameter t depends on the confidence level which is

95 % for a t = 4.3

3.12.2 Experimental Uncertainty on Pore Size Measurement .

A) The nitrogen measurements for the larger pore sizes were performed in duplicate . The instrument gave a deviation of $\pm$ 0.1 Å .

Example : 5.6 $\pm$ 0.1 Å

B) The same method was used for the argon measurements of the smaller pore sizes, and a deviation of $\pm$ 0.1 Å was found .

Example : 4.9 $\pm$ 0.1 Å .

Chapter 4

Results and Discussion

4.1 Desilication

Desilication is a process where removal of the silicon species from the zeolite's framework occurs . Desilication is an extremely important process in the DRS method . DRS is short for : **D**esilication , **R**esilication and **S**tabilization . The desilicated zeolites are termed metastable structures because they could undergo some minor structural changes in order to stabilize their pore network and get a change of their pore size distribution compared to the pore network of the untreated sample .[66] In this first part we will be discussing only the results of the desilicated samples that have been thermally treated at 220 ^{0}C .

It is important in the desilication process to avoid have a decrease of the Si/Al ratio of more than 30 % because any greater change will cause an irreversible collapse of the structure and thus be of no use for any type of application . During the procedure ,the following all three variables are controlled , : 1) temperature of the water bath , 2) initial pH of the solution and 3) the length of time for which the zeolite / alkaline mixture is left in the

water bath . The pH of the alkaline solution was measured to be 11.8, and this is what promotes the breakage of the -[Si-O-Si]- bond . The proposed mechanism for the desilication of the ZSM-5 zeolite is seen in figure 4.1 . We can notice that the two products which are being extracted during the process are : a) sodium orthosilicate (Na_4SiO_4) and its dimer b) sodium pyrosilicate ($Na_6Si_2O_7$) .

We decided to apply the procedure of desilication to four zeolites which have fairly different Si/Al ratios . The DRS method was tested on the NaZSM-5 and the NH_4-ZSM-5 to see what kind of pore distribution would result after desilication and activating the sample at different temperatures , and also to see what kind of pore distribution would result by applying the reinsertion method in coordination with thermal treatment .

As for the Na-X and Na-Y zeolites , only desilication and stabilization were applied to see how this would alter their pore networks and what effects this would have on their cationic exchange capacity .

Other researchers from the Institute Fur Angewandte in Germany , have worked on something that resembles the process of desilication , except that they promoted the removal of aluminum instead of silicon . The aim was to determine the structural and catalytic effects of a post-synthetic sodium

synthetic sodium hydroxide treatment on the H-ZSM-5 zeolite. The application of a strongly basic medium on the one hand represents the conditions of zeolite synthesis , but on the other hand silicates can be dissolved by alkali . This approach consisted of a controlled de- and realumination in order to achieve a catalytic modification by a post-synthetic treatment .[67,68]

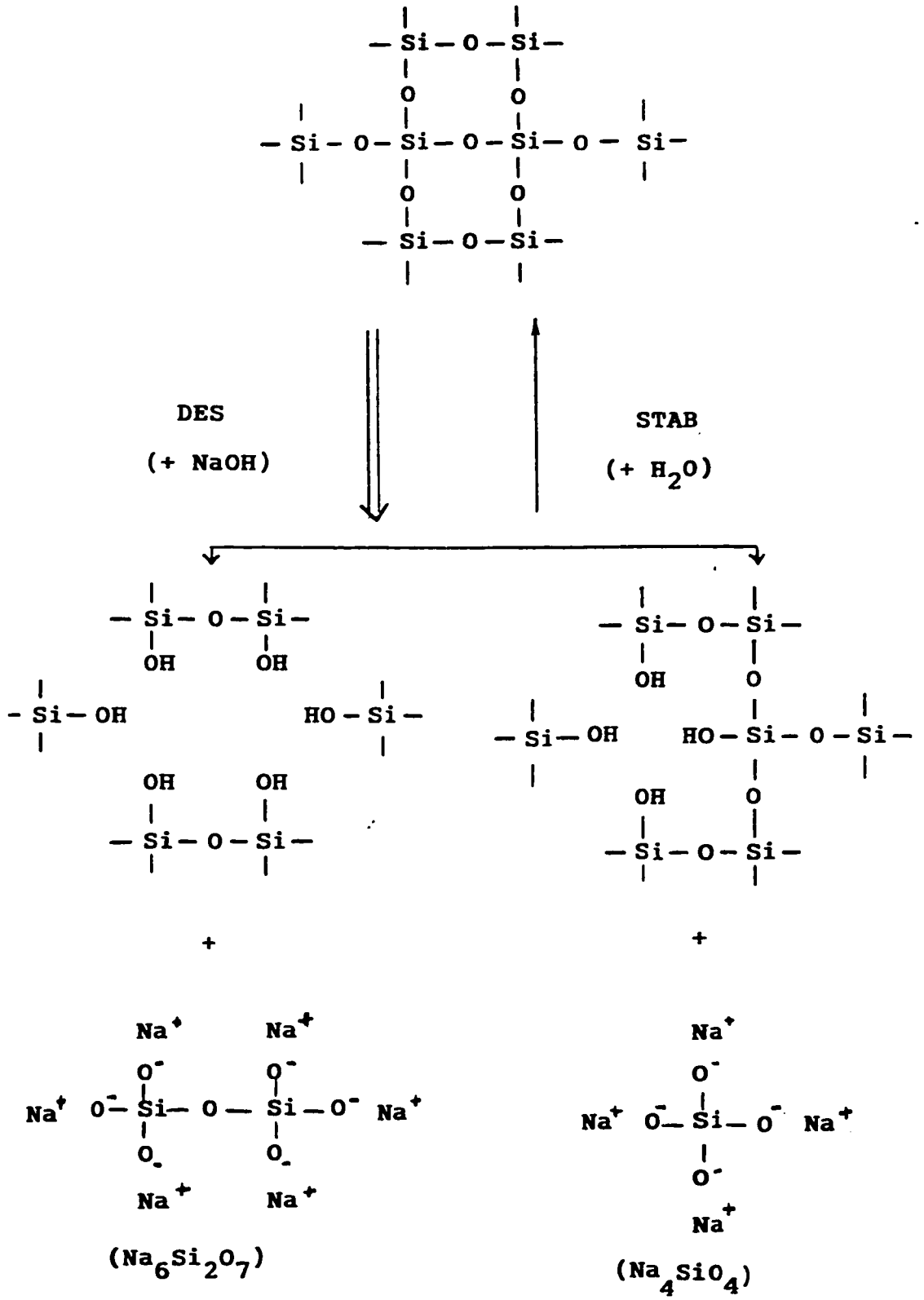

Figure 4.1 Proposed Mechanism for the Desilication of the ZSM-5 Zeolite .

4.2 Chemical Composition

Two types of ZSM-5 zeolites were used in this study ; the first is the ammonium form (NH_4-ZSM-5) which has a Si/Al ratio of 40, and the second is the sodium form which has a lower Si/Al ratio at about 23.1 . Table 4.1, shows the effect that desilication has on the Si/Al and on the Na/Al ratios . Due to previous work which was done in our catalysis laboratory , the optimal treatment for the desilication of the sodium form ZSM-5 was known to be a solution made from 0.8M of Na_2CO_3 and 0.01N NaOH .

Once the desilication was done , it was important to use a few liters of hot distilled water to remove as much of the silica debris that may have been broken off ,but remained loosely held within the pores . Washing with hot distilled water helped remove the ortho and pyro silicates which were been formed by the desilication process . These solutions were kept for later use in the resilication procedure which will be seen in the third part of the results section . Using warm distilled water also helped in reducing the Na/Al ratio closer to unity without changing the Si/Al ratio significantly, by removing as much of the extra sodium which was brought in from the sodium carbonate / sodium hydroxide solution .

Table 4.1 Chemical Composition of the NaZSM5 and the NH_4ZSM5 Zeolites .

Samples	% SiO_2	% Na_2O	% Al_2O_3	Si/Al	Na/Al
NaZSM5	89.7	7.0	3.27	23.3	3.5
DZSM5 (1)	93.0	2.4	4.6	17.1	0.8
DZSM5 (1) (2.5 % ortho)	93.2	2.2	4.6	17.3	0.8
NH_4ZSM5	97.9	0.16	1.9	43.5	0.1
DZSM5 (2)	95.1	2.6	2.3	35.4	1.9
DZSM5 (2) (2.5 % ortho)	93.4	4.3	2.0	40.4	3.6
DZSM5 (2) (0.8M S.C)	94.8	2.6	2.6	30.7	1.7

* Note : (1) Signifies that the sodium form ZSM-5 was used .

(2) Signifies that the ammonium form ZSM-5 was used .

(S.C) means that only sodium carbonate was used for desilication .

The only important result to discuss from table 4.1 is that the Si/Al ratio for the NaZSM5 , compared to the desilicated sample has, decreased by 26.6 % compared to 18.6 % in the case of NH_4ZSM-5 all of them compared to the untreated samples . One would have expected that the zeolite with the highest Si/Al would have a greater change in its Si/Al ratio because of the greater number of silicon atoms, which increases the number and chances of a silicon to be removed. One possible explanation is that the NH_4ZSM5 may need a milder condition with no sodium hydroxide (for example only 0.8M Na_2CO_3) . An attempt was made to see if this new concentration would give us a greater change, and it did because the Si/Al ratio decreased to 30.69, which is a difference of 29 % compared to the non-desilicated sample .

Desilication of Other Zeolites

The sodium form X zeolite has a Si/Al ratio of 1.63 (as shown in table 4.2) , which is a lot smaller than both of the ZSM-5 samples tested . The same mode of treatment for the Na-X, as for the ones having a higher Si/Al ratios, could not be used because to remove the silicon from the Na-X framework requires a greater corrosive action , but at the same time one needs to avoid provoking collapse of the structure . The rule of thumb goes as

follows : the lower the Si/Al ratio , the more alkaline the solution used .For this purpose a solution of Na_2CO_3 / NaOH , which contains more sodium hydroxide than in the case of the ZSM-5, was used . It is important to test different concentrations of sodium hydroxide (0.2N to 0.4N) and see by the characterization results at what limit structural collapse begins to occur. This helped determine the optimal concentration for the Na-X zeolite .

Table 4.2 Chemical Composition of the X- type Zeolite .

Samples	% SiO_2	% Na_2O	% Al_2O_3	Si/Al	Na/Al
Na-X (parent)	52.5	20.1	27.4	1.63	1.21
Na-X (0.2N)	52.3	19.3	28.4	1.56	1.12
Na-X (0.3N)	48.8	21.2	30.0	1.38	1.05
Na-X (0.35N)	47.9	20.3	31.8	1.28	1.05
Na-X (0.4N)	43.1	22.0	34.9	1.05	1.04

As for the Y type zeolite with a Si/Al ratio of 3.17, which is greater than that of Na-X , the conditions for desilication are going to be a lot closer to the X type zeolite than to the ZSM-5 .The concentration of sodium hydroxide used in this case was in the area of 0.1N to 0.3N .

Table 4.3 Chemical Composition of the Y- type Zeolite .

Samples	% SiO_2	% Na_2O	% Al_2O_3	Si/Al	Na/Al
Na-Y (parent)	69.5	12.0	18.6	3.17	1.06
Na-Y (0.1N)	66.4	12.5	21.1	2.67	0.97
Na-Y (0.2N)	65.8	12.7	21.5	2.60	0.98
Na-Y (0.3N)	64.1	11.5	21.4	2.54	0.88

From tables 4.2 and 4.3 ,it is difficult to ascertain which condition is optimal for the Na-X and Na-Y zeolites .Results of some characterization techniques to determine which conditions have brought about an unwanted change in our structure are needed at this point . However , we do notice that there is a gradual decrease of the SiO_2 species, as expected, and that this leads to a normal decrease in the Si/Al ratio .

Zeolites are porous materials where pore structure and the surface area are related to each other . Both the total surface area and the pore size distribution can be determined from the physical adsorption - desorption of nitrogen. After performing the procedure of desilication and heating (220 ^{0}C) ,the surface and micropore area ,micropore volume and diameter, changed for both samples of ZSM-5 . If the desilication procedure was too harsh one would expect to see a large decrease in surface area, which would indicate a structural collapse .

Micropore size distribution by adsorption of argon was used to characterize samples that were heated at temperatures of 220 ^{0}C and above , but more interesting results were obtained for samples that were heated at 550 ^{0}C . The data interpretation of Horvath and Kowazoe, with the interaction parameter of 4.9 x 10^{-43} erg / cm^{4}, were used for the determination of the peak maxima for the micropore size distribution .

Table 4.4 Textural Properties for the NaZSM-5 heated at 220 °C .

Samples	Surface Area (sq.m/g)	Micropore Area (sq.m/g)	Micropore Volume (cc/g)	Diameter max. (A^0)
NaZSM5 (parent)	341	242	0.10	1)5.2 * 2) 4.9
DZSM5 (1)	391	290	0.12	1) 5.4 * 2) 4.7
DZSM5 (1) (1% ortho)	397	301	0.12	1) 5.0 * 2) 5.6
DZSM5 (1) (2% ortho)	305	219	0.09	1) 5.1 * 2)5.3
DZSM5 (1) (2.5% ortho)	275	213	0.09	1) 5.4 * 2) 4.9
DZSM5 (1) (3% ortho)	338	255	0.10	1) 5.6 * 2) 5.0
DZSM5 (1) (5% ortho)	358	296	0.12	1)5.4 * 2) 5.1

N.B see table 4.1 page 96 .

*where in the diameter maximum measurements , the * means that the peak had the largest volume of the two peaks measured .*

Table 4.4 , shows that after desilication and thermal treatment at 220 ^{0}C , the surface area and the micropore area have also increased considerably . This could be explained by the fact that micropores are being formed in greater number after desilication .An increase in the micropore volume after desilication is also observed . The diameter of the micropores formed gave two peaks each : one at 5.2 Å and another smaller one at 4.9 Å for the parent, giving us an average of 5.1Å . After the desilication treatment , the largest peak shifted towards a larger value at 5.4 Å, whereas the smaller peak shifted from 4.9Å to the smaller value of 4.7 Å. It was found that when the samples were heated at 220 ^{0}C , the framework of the desilicated zeolite did not undergo any stabilization . The goal was to get a more uniform micropore size distribution, which is not really the case for samples heated at this temperature . This method enables one to enlarge the micropores compared to their initial size in the parent . A question now arises as to whether these dimensions remain the same after heating at higher temperatures or shift to larger values ?

Table 4.5 Textural Properties for the NH_4ZSM-5 heated at 220 ^0C .

Samples	Surface Area (sq.m/g)	Micropore Area (sq.m/g)	Micropore Volume (cc/g)
NH_4ZSM5 (Parent)	470	310	0.13
DZSM5 (2)	352	273	0.11
DZSM5 (2) (1% ortho)	394	301	0.12
DZSM5 (2) (1.5% ortho)	392	293	0.12

* see table 4.1 page 96 .

Results were obtained using an acidic type of ZSM-5 . The proton form is known to have an effect on the structure's surface area because of the fact that it still contains some acidic sites. This would explain why the surface and micropore area decreases after desilication .

Table 4.5 shows that after desilication , a considerable decrease in the surface and micropore area occurs . This explains why a decrease of the micropore volume measured after desilication is also observed .

4.4 Thermal Treatment

During the desilication process, there is a controlled removal of some silicon species from the zeolitic framework which is treated . An important aspect which will be discussed in this second part of the results section is the effect that thermal and steam treatment have on the stabilization and healing of the desilicated framework . The most important aspects to note will be the differences in the micropore size distribution caused by these treatments .

The micropore size distribution of the steamed desilicated zeolite was identical to that obtained when the desilicated material was treated only in air at very high temperatures [60] . As hypothesized by Scherzer based on the observations of Kerr , the framework of dealuminated or desilicated zeolites may undergo some stabilization changes owing to the reaction of silanol groups (formed by the removal of Al or Si from the framework) with silica containing debris in the presence of steam . [59,60,63] Breck also showed that this stabilization process is the replacement of the 4 protons (from the four Si-OH groups) in the tetrahedral positions by silicon introduced as $Si(OH)_4$ .This is the species that is responsible for the transport of silica in the water vapor at high temperatures and may originate from a small amount of decomposed zeolite . There was some controversy at the time of the publication of the

papers by Kerr and Breck, as well as that of Skeels and Breck , the latter dealing with isomorphous substitution of Al .[63]

The materials they used for the Y zeolite were not sufficiently modified because of the relatively limited extent of dealumination observed during the Y zeolite ultrastabilization . In our case , the changes in the chemical state within the zeolite framework are important , thus resulting in larger variations of some properties such as the pore size and pore-size distribution of the zeolite .It was discussed earlier that during desilication, the silica -containing debris were sodium orthosilicate and its dimer sodium pyrosilicate .

The thermal treatment may be the reverse reaction of desilication . However for such a framework stabilization only a small number of Si vacancies were involved . The process requires some sodium orthosilicate and / or sodium pyrosilicate which are still present in some locations next to the silanol groups . Water will surely act as a carrier because its use results in a lower treatment temperature in the steaming process . [66]

The characterization results that have been achieved by the procedure of desilication in coordination with thermal treatment of the NaZSM-5 , NH_4-ZSM-5 and the faujasites (Na-X and Na-Y) will be discussed in part 4.5 .

4.5 Surface Area Measurement

The following tables present the results obtained by heating the desilicated samples to higher temperatures .These allow an analysis of the changes brought to the samples' micropore size distribution compared to the non treated (parent) sample heated at the same temperature . Both types of ZSM-5 zeolites were analyzed to see how they would be changed by thermal treatment . The other two samples analyzed were the Na-X and Na-Y zeolites . The aim was to see how the thermal treatment would change their pore sizes and if it would improve their cationic exchange capacities .

Table 4.6 Textural Properties for the NaZSM-5 heated at 550 ^{0}C .

Samples	Surface Area (sq.m/g)	Micropore Area (sq.m/g)	Pore Volume (cc/g)	Diameter max. (A^0)
NaZSM5 (parent)	401	292	0.32	1)5.2* 2)5.4
DZSM5 (1)	407	296	0.36	5.5
DZSM5 (1) (1% ortho)	397	301	0.36	1)5.4* 2)5.8
DZSM5 (1) (2% ortho)	303	219	0.31	1)5.0* 2)5.3
DZSM5 (1) (2.5% ortho)	333	251	0.31	4.9
DZSM5 (1) (3% ortho)	320	239	0.31	5.3
DZSM5 (1) (3.5% ortho)	296	234	0.30	1)5.2 * 2)5.6
DZSM5 (1) (4% ortho)	302	232	0.30	1)5.3* 2)5.5
DZSM5 (1) (5% ortho)	286	212	0.31	1)5.4* 2)5.7

In table 4.5 , one can note that the parent sample has two peaks; one at 5.2 Å and one at 5.4 Å, which average out to a value of 5.3 Å . Comparing this to the same sample which was heated at 220 ^{0}C (see table 4.4) , one sees that the surface and micropore area have increased with a higher thermal treatment . The sample heated at 220 ^{0}C also has two peaks : one at 5.2 Å and another at 4.9 Å, which gives an average of 5.1 Å . There is an increase of 0.2 Å of the pore size with an elevation in temperature from 220 ^{0}C to 550 ^{0}C.

As for the desilicated samples one notes that the surface and micropore areas have remained similar to its parent . But comparison of the desilicated sample heated at 220 ^{0}C (see table 4.4) and the one heated at 550 ^{0}C,shows that there is a very small increase in the surface and micropore areas . The sample heated at 550 ^{0}C showed a strong peak at 5.5 Å and the sample heated at 220 ^{0}C had two peaks : one at 5.4 Å and another at 4.7 Å, which average out to 5.1 Å . So again, one sees that by heating to a higher temperature , an increase of the pore diameter by 0.4 Å occurs , while the surface and micropore area remain very comparable to that of the parent heated at the same temperature .

This may be a very useful technique , for any process which requires a

This may be a very useful technique , for any process which requires a larger pore size . What is primordial is that the sample does not loose any of its surface area when it is heated to high activation temperatures. It is noticed also that heating to 550 ^{0}C has the effect of stabilizing the framework and thus plays a key role in the improvement of the micropore size distribution .

Table 4.7 Textural Properties For the NH_4-ZSM-5 heated at 550 C .

Samples	**Surface Area (sq.m/g)**	**Micropore Area (sq.m/g)**	**Pore Volume (cc/g)**	**Diameter max. (A^0)**
NH_4-ZSM-5 (parent)	406	260	0.26	1)5.0 * 2) 5.9
DZSM-5 (2)	362	244	0.33	1)5.0 * 2) 5.6
DZSM-5 (2) (1.5% ortho)	360	251	0.30	5.7
DZSM-5 (2) (2.5% ortho)	330	234	0.27	4.9

Table (4.7) , shows that the surface and micropore areas have

Table (4.7) , shows that the surface and micropore areas have decreased very gradually in going from the parent to the treated samples. As for the diameter of the micropores , a decrease of the average value from the parent (5.5 Å) to the desilicated value of (5.3 Å) was observed . One also notices a slight increase to 5.7Å for the sample treated with 1.5% orthosilicate . After treatment with 2.5% orthosilicate, the results show that the diameter had shrunk to 4.9 Å, and that only one peak is present .

Table 4.8 Textural Properties Using Nitrogen For the Na-Y Zeolite heated at 450^{0}C.

Samples	**Surface Area (sq.m/g)**	**Micropore Area (sq.m/g)**	**Micropore Volume (cc/g)**	**Average Pore Diameter (A^0)**
Na-Y	673	627	0.29	14.7
Na-Y (0.1N)	694	645	0.30	14.8
Na-Y (0.2N)	636	591	0.27	14.8
Na-Y (0.3N)	573	532	0.25	15.1

Table 4.9 Textural Properties Using Nitrogen For the Na-X zeolite heated at 450 °C.

Samples	Surface Area (sq.m/g)	Micropore Area (sq.m/g)	Micropore Volume (cc/g)	Average Pore Diameter (A^0)
Na-X	516	479	0.22	15.0
Na-X (0.2N)	513	479	0.22	15.0
Na-X (0.3N)	591	553	0.26	15.0
Na-X (0.35N)	641	600	0.28	14.9
Na-X (0.4N)	514	477	0.22	15.1

Table 4.8 shows that the 0.1N sodium hydroxide treatment increases the surface and micropore area as well as the average pore diameter, when compared to the non-treated sample . After treatments with 0.2N and 0.3N NaOH , a gradual decrease in the surface and micropore area is observed compared to the Na-Y treated with 0.1N for sodium hydroxide . As for the pore diameter, the value is seen to really change only once the sample has been treated with a 0.3N concentration . It goes from 14.8 Å to 15.1 Å , due to the corrosive action of the NaOH which increases the pore openings .

Table 4.9 , indicates that the trend is somewhat different from what is

given in table 4.8 . The treated Na-X surface area has increased compared to the parent (untreated), and it reaches a maximum value of 0.35N. The micropore area and the micropore volume also follow the same trend, and a maximium was established at the same concentration .One important point worth noting is that the average pore diameter seems to decrease after treatment at low concentrations of sodium hydroxide . The minimum pore diameter was reached at 0.35N which seems to indicate that the majority of pores formed are micropores and very little mesopores or macropores . We could also note that at the highest concentration (0.4N) , the surface and micropore area and micropore volume decreases, which tells us that this condition is becoming too harsh for the zeolite material and that a concentration of 0.4N is excessive in the case of the Na-X sample .

From tables 4.8 and 4.9 ,conclusions are that the optimum conditions differ for both the Na-X and Na-Y zeolites , as expected . This may be explained by the fact that the Na-X has a lower Si/Al ratio and resists to tougher conditions , whereas the Na-Y and its high Si/Al ratio require a weaker alkaline condition . The optimal sodium hydroxide concentration at 450 ^{0}C was found to be 0.35N for Na-X and at 0.1N for Na-Y .

4.6 MAS - NMR (^{29}Si and ^{27}Al)

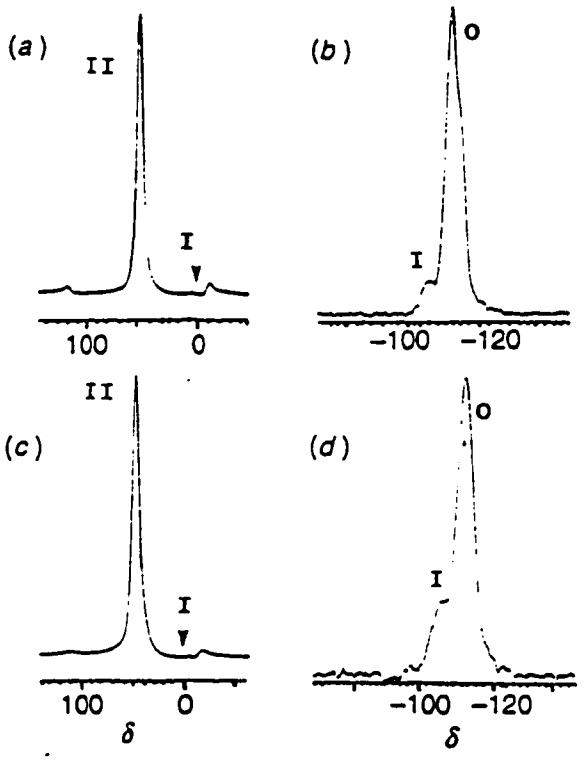

Figure 4.2 ^{27}Al MAS-NMR Spectra of : (a) Parent ZSM-5 and (c) ZSM-5/TW ; and ^{29}Si MAS-NMR spectra of: (b) Parent ZSM-5 and (d) ZSM-5/TW.

In figure 4.2 , the chemical shift is given with respect to the $Al(OH)_6^{3+}$ for ^{27}Al . Signal (I) is the aluminum which is extra lattice and is known to have an octahedral configuration , whereas the second signal (II) is the aluminum which is within the lattice and has a tetrahedral configuration . This indicates that desilication does not affect the aluminum sites in any way because the signals have not changed compared to the parent .

Parts (b) and (d) of figure 4.2 deal with the number of aluminum which are around the central silicon , the chemical being given with respect to TMS which is set at 0 ppm . In this case there is little difference between the parent ZSM-5 and the desilicated zeolite . The zero signal means that there is four silicons around the central one .Signal (I) means that there are one aluminum and three silicons around the central one, and so on for the other signals (II, III and IV) .The only change observed is, that by performing desilication ,there is an increase in the proportion of one aluminum around the central silicon which is normal because desilication brings about the removal of silicon which is replaced by an aluminum, and this was proven by the ^{29}Si MAS-NMR spectrum results .

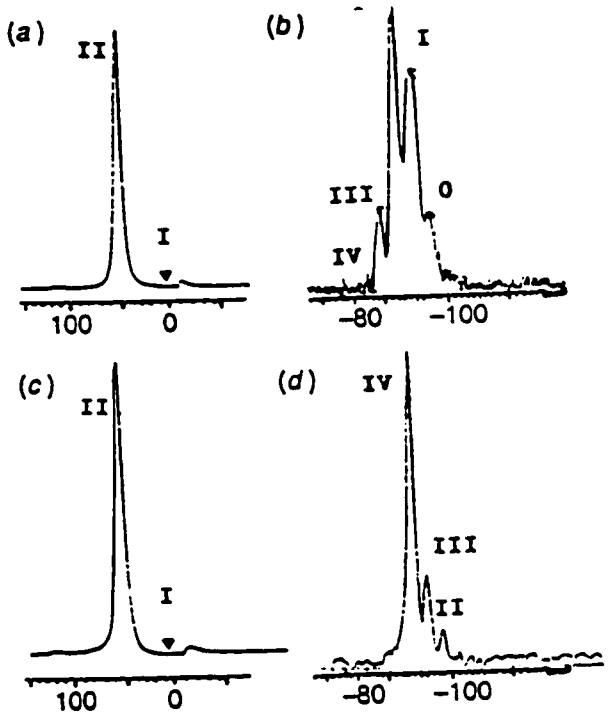

Figure 4.3 ^{27}Al MAS-NMR spectra of : (a) Parent Na-Y and (c) Na-Y/TW ; and ^{29}Si MAS-NMR spectra of : (b) Parent Na-Y and (d) Na-Y/TW.

The solid - state NMR data of figure 4.3 shows no changes occur at the aluminum sites ,for the same reasoning given in discussion of figure 4.2. As for the ^{29}Si MAS-NMR ,an increase is observed in the number of aluminum neighbors for the silicon sites in going from the parent to the desilicated sample .This is expected because the Si/Al ratio is at about 2.6 , so they possess some silicon which can be broken off and replaced by aluminums .

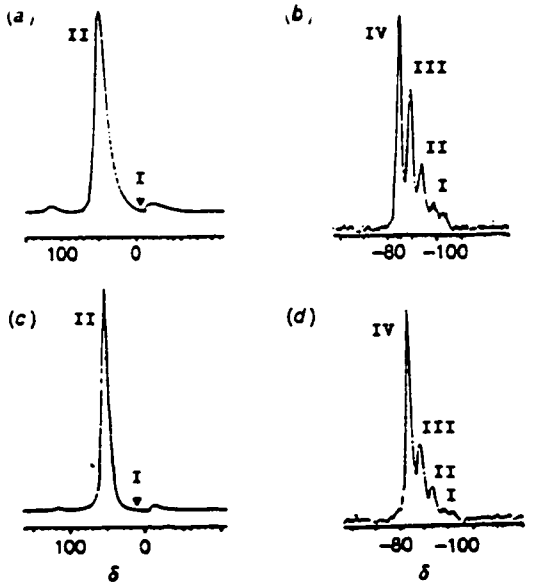

Figure 4.4 ^{27}Al MAS-NMR spectra of : (a) Parent Na-X and (c) Na-X/TW ; and ^{29}Si MAS-NMR spectra of : (b) Parent Na-X and (d) Na-X/TW .

In the case of the MAS-NMR for the Na-X zeolite shown in figure 4.4 , one notices that there is some difference in the ^{29}Si NMR spectra before and after desilication . The signal with four aluminums around the silicon for the parent remains almost unchanged for the desilicated sample,except for a small decrease in the proportions of all four signals .The signal with four aluminums around the silicon is present because of the low Si/Al ratio, and desilication just increases the proportion of that signal at the expense of the 3 others, where each of them lose some of their signal . As for the aluminum there is no change between the octahedral one (signal I) and the tetrahedral one (signal II), before and after desilication , showing that the aluminums were not affected during the desilication process .A change is however observed between the Na-X an Na-Y MAS-NMR , and this is due to the lower Si/Al ratio of the Na-X which is at 1.5 .

4.7 X-Ray Powder Diffraction

For the powder diffraction , the treated and untreated zeolites heated at the same temperature were compared and the analysis were always done on the same day .The region scanned was in the $2\theta = (7.0 - 50.0)^0$ region (see figures 4.5) . The area where the relative intensities could be influenced in the region of 2θ ($22.5\text{-}25.0\ ^0$) [69,70]

The degree of crystallinity is calculated by taking the peaks of the non-treated sample in this region and doing the same for the treated sample . We then apply the following equation :

$$\% \text{ Crystallinity} = \Sigma \text{ intensities (treated)} / \Sigma \text{ intensities (untreated)} \times 100$$

Table 4.10 Chemico-Physical Properties of NaDZSM-5 samples activated at 550 ^{0}C.

Zeolite Samples	Degree of Crystallinity (%)
NaZSM-5 (Parent)	100
NaDZSM-5	88.6
NaDZSM-5 (2.5% ortho)	85.8
NaDZSM-5 (2.5% meta)	81.6

Table 4.10 ,indicates only a slight difference between the parent zeolite and the desilicated samples . A difference of only 11.4% was observed between both samples . Additional proof that the structure did not change dramatically between both samples is that the BET sample results showed no significant variations of the surface area . The small loss of crystallinity should not be ascribed merely to a partial structural collapse upon heating at high temperatures.

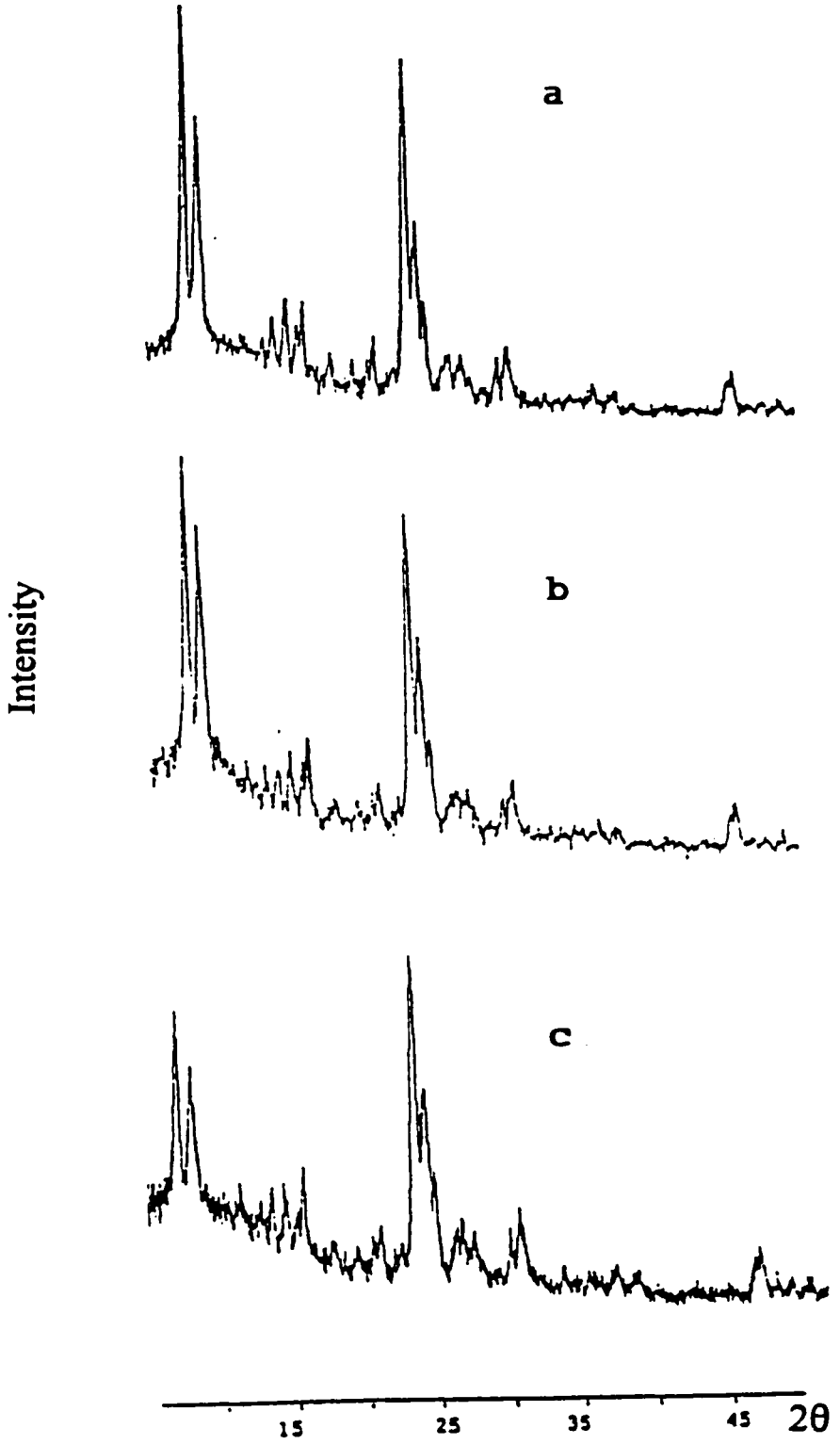

Figure 4.5 X-ray diffraction patterns of : a) ZSM-5 , b) DZSM-5 and c) DZSM-5 (2.5% ortho) .

Table 4.11 Chemico-Physical Properties of Na-X samples activated at 450 ^{0}C.

Zeolite Samples	Degree Crystallinity (%)
Na-X (Parent)	100
Na-X (0.2N)	86.4
Na-X (0.35N)	80.4
Na-X (0.4N)	82.4

Table 4.12 Chemico-Physical Properties of Na-Y samples activated at 450 ^{0}C.

Zeolite Samples	Degree Crystallinity (%)
Na-Y (Parent)	100
Na-Y (0.1N)	88.7
Na-Y (0.2N)	86.5
Na-Y (0.3N)	91.4

Peak intensities are known to vary with the degree of hydration of the samples . Keeping this in mind only samples treated at the same temperature 450 ^{0}C were compared . All samples showed a reasonable decrease in the degree of crystallinity such that no structural degradation is believed to have occurred .The overall structure for the treated samples remained the same even after there was a significant decrease in the Si/Al ratio . In table 4.12 , one notices something which at first glance should not have occurred , the value of 91.4% for the Na-Y with 0.3N of NaOH . To explain this value , first of all it should be noted that an average difference of 15-20 % between the treated and non-treated samples is observed with respect to their crystallinity . This may be due to factors such as humidity , temperature and orientation of the powder crystals which are known to cause variations in the intensities . Examining the BET results (table 4.8) for the Na-Y zeolite treated with 0.3N of sodium hydroxide , one notices a decrease in the surface area which means that some minor collapse has occurred , making it impossible to get such a high value for the DC (%) results. So because both results contradict each other, and because the BET results are more precise , there appears to be some structural change within the treated sample at this concentration .

4.8 Steam Treated Samples

Table 4.13 Textural Properties of Na-Y samples after thermal or Steam Treatment.

Zeolite Samples	Surface Area (Sq.m/g)	Maximum Pore Volume (cc/g)	Median Pore Diameter (A^0)
Parent 550 C	735.1	0.26	7.4
Y (0.1N) 550 C	722.2	0.25	7.4
Y (0.2N) 550 C	714.1	0.24	7.3
Y (0.3N) 550 C	738.3	0.25	7.2
Y (0.3N) 650 C	722.0	0.25	7.3
Y (0.2N) 120 C	661.5	0.23	7.3
Y (0.2N) steam 400 C	706.1	0.24	7.3
Y (0.3N) steam 300 C	731.7	0.25	7.3

The above table shows that heating at higher temperatures brings about a constant value in the case of surface area .What is more important to note is that the steaming process has the tendency to heal the zeolite framework . Looking at the value for the Na-Y sample treated with 0.3N of

NaOH and heated at 550 ^{0}C ,it shows little difference with that observed after steam treatment of the sample at 300 ^{0}C . This explains the fact that the heating is decreased from 550 ^{0}C by using steam . This method would give the same results as thermal treatment, without taking any chances of provoking a partial collapse of the structure due to the higher temperature . Even heating the sample at 650 ^{0}C does not give us as large a value compared to the steam treatment at 300 ^{0}C .

Table 4.14 Textural Properties of Na-X samples after thermal or Steam Treatment.

Zeolite Samples	Surface Area (Sq.m/g)	Maximum Pore Volume (cc/g)	Median Pore Diameter (A^0)
Parent 550 C	571	0.25	7.4
X (0.2N) 550 C	616	0.21	7.2
X (0.3N) 550 C	600	0.21	7.4
X (0.35N) 550 C	601	0.21	7.4
X (0.4N) 550 C	619	0.21	7.4
X (0.3N) 650 C	606	0.21	7.4
X (0.35N) 650 C	634	0.22	7.3
X (0.4N) 120 C	643	0.21	7.4
X (0.2N) steam 300 C	314	0.10	7.4
X (0.3N) steam 300 C	417	0.14	7.4

The table above shows that heating the treated Na-X samples above 650 ^{0}C will not decrease the surface area of the samples . This is proof that heating above 550 ^{0}C will not initiate some structural collapse of the structure

.

An attempt was made to see if steaming at a lower temperature would give us the same results as thermal treatment . The values obtained with steaming were close to 50% lower than the ones obtained with the thermal treatment. One possible reason for this may be that the Si/Al ratio being lower , less silica species has been removed , so a higher temperature than 300 ^{0}C is needed during steam treatment to help heal the sample by transporting silica to areas of the structure that need it and get a considerable increase in the surface area.

Need For Stabilization (Framework Healing)

The results presented in this section indicate that when talking about desilication/stabilization (DS) or desilication/ resilication/ stabilization (DRS) , the most important step in this whole process is the stabilization using high temperatures . Breck discusses the fact that enhanced stability at high temperatures and under hydrothermal conditions of the stabilized zeolites is of considerable significance [31,59,72] . He concluded that the stabilization process applied to the ammonium form of the zeolite is a process of controlled thermal decomposition and dehydroxylation . As a result of the dehydroxylation process , framework defects which are considered minor

because they are very localized may be present . He found that subsequent heat treatment in a hydrothermal atmosphere may cause some silica, which comes from small portions of degraded zeolite , to take positions in the vacant tetrahedral sites and reconstruct the framework and this has been found to promote a reduction in the size of the unit cell . In our case , an attempt was made to take his observations one step further by provoking major defects generalized across the framework and then see how the structure would react to heat stabilization .[72,73,74]

4.9 Cationic Exchange Capacity

The ion exchanging properties of zeolites were first reported in the middle of the 19th century by Thompson , Way and Eichhorn . Thus , Eichhorn investigated the exchange of Na^+ for Ca^+ by the Chabazite/Natrolinite system . However , it was not until 50 years later that this aspect of zeolite chemistry was applied industrially .Water softening and removal of disturbing metal ions from boil feed-water are essential in the generation of steam . This became more and more important at the time when industrialization was growing fast .[74,75,76,77,78]

Zeolites are very effective for ion-exchange because of their overall stable and solid framework . They are stable with regards to high temperatures , oxidizing/reducing agents , ionizing radiation , physical attack by swelling .

Compared to organic ion-exchangers , zeolites have many advantages such as : 1)being more stable at elevated temperatures , 2) they are not attacked by ionizing radiation and 3)they are considerably more selective in certain separations .

Zeolites are well suited for ion exchange mainly because of their selectivity which is a consequence of their molecular sieve property .

For instance big cations cannot diffuse into channels and cavities of small pore zeolites . If two cations - one larger , the other smaller than the pore entrance -interact with a zeolite, only the smaller one will be exchanged . Ion exchange reactions are mostly always done in aqueous solution . For this reason hydration must be taken into account when cations sizes are compared. Depending on the charge density of the cation the hydrating water molecules are bound more or less strongly . If the cations can pass the zeolite pores only after having lost the water molecules coordinated to them in solution , a distinct kinetic effect is observed , which varies with the ionic hydration energies .

Zeolites are a very useful as builders in detergents where they replace the phosphates .The problem with phosphates is that they are non-toxic to humans and aquatic life but they produce a phenomena in the water streams called eutrophication . It brings about a negative effect on the functionability of the ecological system and the production of drinking water. This phenomena is mostly due to an excessive concentration of phosphates in our lakes and rivers . Detergent manufactures have tried to find ways to replace phosphates by a suitable detergent builder . The way this builder would work is by reducing the hardness of water , which means that it performs the

complexation of the Ca^{2+} and Mg^{2+} ions . These are the requirements that the detergent builder should have : 1) no decrease in detergent quality , 2) toxicological and ecological harmlessness , 3) economical application and 4) large-scale production from easily available raw materials . So the first task of any zeolite is to remove the calcium and magnesium ions and heavy metal ions by ion exchange for soft sodium ions .

Another very useful application of zeolites is in the separation of radioisotopes . They have a higher stability to radioactive radiation , and they are more resistant to aqueous solutions at elevated temperatures .

Here are some results obtained for the ion-exchange capacity of the Na ZSM-5 treated and untreated . Tests were also done with the Na-X , Na-Y zeolites compared to each other and then compared to the Na-A zeolite which has some differences compared to the two previous ones .

Table 4.15 Ion Exchange Activity of the zeolite samples treated at various Temperatures .

Samples	Initial rate (r_0 , ppm/min)	Ca^{2+}(ppm) removed after 30 min.	Averg. Value	Δ (%)*
Parent 110 °C	-4.7	21.9		
Parent 300 °C	-6.8	20.2	21.6	
Parent 450 °C	-8.5	22.7		
Desilicated 110 °C	-4.8	28.1		
Desilicated 150 °C	-7.2	27.6		
Desilicated 200 °C	-5.2	26.5	27.4	27
Desilicated 250 °C	-6.4	27.0		
Desilicated 300 °C	-7.0	27.6		
Desilicated 350 °C	-9.2	34.2		
Desilicated 450 °C	-11.4	39.9	36.7	70
Desilicated 550 °C	-11.5	35.9		

* compared with the parent zeolite .

Table 4.15 , shows that the average removal of calcium seems to increase slightly with heating of the parent ZSM-5 zeolite . There was a much larger increase in the value after the sample was desilicated and heated up to 300 ^{0}C . An increase of 27 % was observed as compared to the average value of the parent. Once the sample was heated to 550 ^{0}C the removal increased even more and the difference with the parent was of 70 % .It is obvious that desilication and thermal treatment to high temperatures have shown an improvement in its effectiveness to remove calcium . It is know that the pore size increases with desilication and thermal treatment and that this is the main reason why an improvement in the ion exchange activity is observed . [79]

Table 4.16 Ion removal and some physico - chemical properties of Na-X , Na-Y and Na-A .

Samples	Si/Al	CEC (millieq./g)	Pore size (A^0)
Na-A	1.00	7.16	4.2
Na-X	1.56	6.41	7.4
Na-Y	2.67	4.45	7.4

Table 4.17 The removal of calcium and magnesium ions and the total removal .

Temp.^{0}C	Na-A			Na-X			Na-Y		
	I.R Ca %	I.R Mg %	I.R Total %	I.R Ca %	I.R Mg %	I.R Total %	I.R Ca %	I.R Mg %	I.R Total %
25	92.5	24.3	69.8	71.8	52.5	65.0	69.6	46.0	61.7
45	74.9	59.2	69.7	75.0	69.7	73.2	68.2	66.8	67.7
65	80.2	83.4	81.2	81.0	80.0	80.7	68.0	63.0	66.3

where I.R is the ion removal .

Table 4.16 ,shows that the zeolite with the lowest Si/Al ratio, in our

case the Na-A zeolite , has the greatest extent of cationic exchange capacity (CEC) , while at the same time offers the smallest pore size of all the tested materials .

Table 4.7 gives more information on the effectiveness of each zeolite in the removal of calcium and magnesium ions, as well as the total ion removal . At 25 ^{0}C ,the effectiveness was as follows : Na-A > Na-X > Na-Y , mostly due to the fact that it is dependant on the Si/Al ratio .There was an improvement of the total ion removal (I.R) for the Na-X at a higher temperature. At 65 ^{0}C the following sequence was found : Na-A = Na-X > Na-Y .

At ambient temperature the magnesium ion removal was identical to the cation exchange capacity .It was found that this changes at a higher temperature to give us the following sequence : Na-A << Na-X < Na-Y . This could be explained by the zeolites' pore size as seen in table 4.16 . Although Na-A is known to be a highly efficient insoluble ion exchanger capable of removing calcium ions , its removal efficiency for magnesium ions is low , particularly at ambient temperature when its exchange rate is low . [75]

The enhanced cation exchange capacity of the desilicated Na-X is

herein demonstrated to be an important property , rendering it even more effective in the removal of calcium and magnesium ions from wash water than the Na-A zeolite commercially used in detergent powders . [72]

In conclusion it is noted that at ambient temperature , the initial rate of calcium and magnesium removal determined for the large pore-sized zeolites X and Y were much higher than those determined for the small pore-sized zeolite Na-A . The initial rate for the removal of magnesium ions did not change significantly with temperature when the Na-X and the Na-Y zeolites were used . There was, however, an important variation for such a parameter when the Na-A zeolite was used . This may suggest that the ion-exchange rate with magnesium ions was strongly dependent on the diffusion rate of these ions through the narrow pores of the Na-A zeolite . Such diffusion limitations for the Na-A zeolite , at least at ambient temperature , were due to the strong solvation tendency of magnesium ions, which could form bulky complex ions with water molecules . However at higher temperatures , there was a significant improvement in the diffusion rates of Mg^{2+} through the pore system of the Na-A which finally resulted in an improvement performance for ion removal . On the other hand , since the Na-X and Na-Y zeolites had the same open structure but different cation exchange capacity , they exhibited

significantly different values for the total-ion removal .

It has been noted that a mixture of zeolites X and A have been claimed to exhibit synergistic effects in the removal of Ca^{2+} and Mg^{2+} from hard water . [72]

4.10 Reinsertion of the (Si-O) Species

As stated earlier , desilication was a very important step to get the removal of silicon species (sodium orthosilicate and sodium pyrosilicate) from the framework . It has been shown that the removal of the silicon species, which is very selective in its action, cannot bring about a change in the Si/Al ratio of more than 30 % because this would provoke an irreversible structural collapse or loss of the very important Al tetrahedral sites .Upon thermal treatment of this treated sample an enlargement of the pore size compared to the parent sample was observed .

An attempt was made to reinsert a small portion of the silicon species removed, from 1-5 % Wt. (see table 4.18), and see how this would change the pore dimensions .The hypothesis being that if the removal was selective, then the reinsertion should also be selective, and adding a smaller amount than what was removed would place the inserted species in very strategic areas within the framework .

Table 4.18 Amounts of (Si-O) species used for the reinsertion operation with 5 grams of desilicated sample .

Desilicated Zeolites	Amount of (Si-O) species in grams .	Weight % of (Si-O) added.
NaDZSM-5	0	0
NaDZSM-5 (1.0)	0.050	1.0
NaDZSM-5 (2.0)	0.100	2.0
NaDZSM-5 (2.5)	0.125	2.5
NaDZSM-5 (3.0)	0.150	3.0
NaDZSM-5 (3.5)	0.175	3.5
NaDZSM-5 (4.0)	0.200	4.0
NaDZSM-5 (4.5)	0.225	4.5
NaDZSM-5 (5.0)	0.250	5.0

Table 4.18 shows how small the amounts of silicon species added were .It is interesting to see how the results of the micropore size and the surface area changes within the range of (1-5% Wt.) of silicon species .

In table 4.1 (chemical composition) ,it was shown that we could notice that for both types of ZSM-5 zeolites , adding an amount of (Si-O) species of 2.5 % Wt , for example , brings about an increase of the SiO_2 species and an overall increase in the Si/Al ratio . In the case of the sodium form ZSM-5 ,

the increase was of 1.2% between the desilicated and resilicated species , but for the ammonium form ZSM-5, that increase was much larger at 14.1 % . This may be due to the fact that having a larger Si/Al ratio , more silicon species may be removed so that once it is reinserted more of it gets used within the structure .

In table 4.4 , the results at 220 ^{0}C show that the surface area and the pore volume decreased until it reached 2.5 % orthosilicate insertion and then went back up when it reached 5% of the Si-O species . As for the size of the pores formed ,there are two peaks which would indicate that at this temperature the distribution is not optimal (see fig. 4.10) . One wants a distribution that gives one sharp peak indicating that the pore sizes are almost all within the same size .

A large difference was noticed in the results for both types of ZSM-5 zeolites after heating at 550 ^{0}C (see table 4.6 & 4.7) compared to the ones heated at 220 ^{0}C (see fig. 4.9) . It can be seen that the surface area and the pore volume decreased gradually with increasing amounts of (Si-O) species inserted . It affects both the micropores (surface area of micropores) and the other pores (total surface area) . The parent zeolite for the sodium form gave a peak at 5.3 Å (Fig. 4.6) as expected . After desilication , the peak had

increased to 5.5 Å (fig.4.7) . Addition of 2.5 % Si-O species to give NaDZSM-5 , gave a strong peak at 4.9 Å (fig.4.8) , while the NaDZSM-5 (5.0) exhibited a strong peak at 5.7 Å (fig.4.10) .

The same trend could be seen with the ammonium form ZSM-5 . The NaDZSM-5 (2.5) shows a minimum peak at 4.9 Å ,which indicates that both types of ZSM-5 react in the same fashion to the addition of a small amount of (Si-O) species .

In figure 4.12, which is a general view of the variation of the micropore size distribution following the reinsertion of (Si-O) species versus the diameter in angstroms . It is very surprising that while the surface area and pore volumes decreased gradually with increasing (Si-O) loading , the pore size went through a minimum at 2.5% loading and increased as the loading got higher . This is irrefutable evidence that the (Si-O) species is not just deposited onto the surface of the desilicated zeolite , otherwise the micropore size would decrease with increasing (Si-O) loading . The reproducibility of these materials in terms of the size for the newly formed micropores , thus suggests some specific interaction of the reinserted species with the silicon vacancies of the framework of the desilicated zeolite during the stabilization treatment .

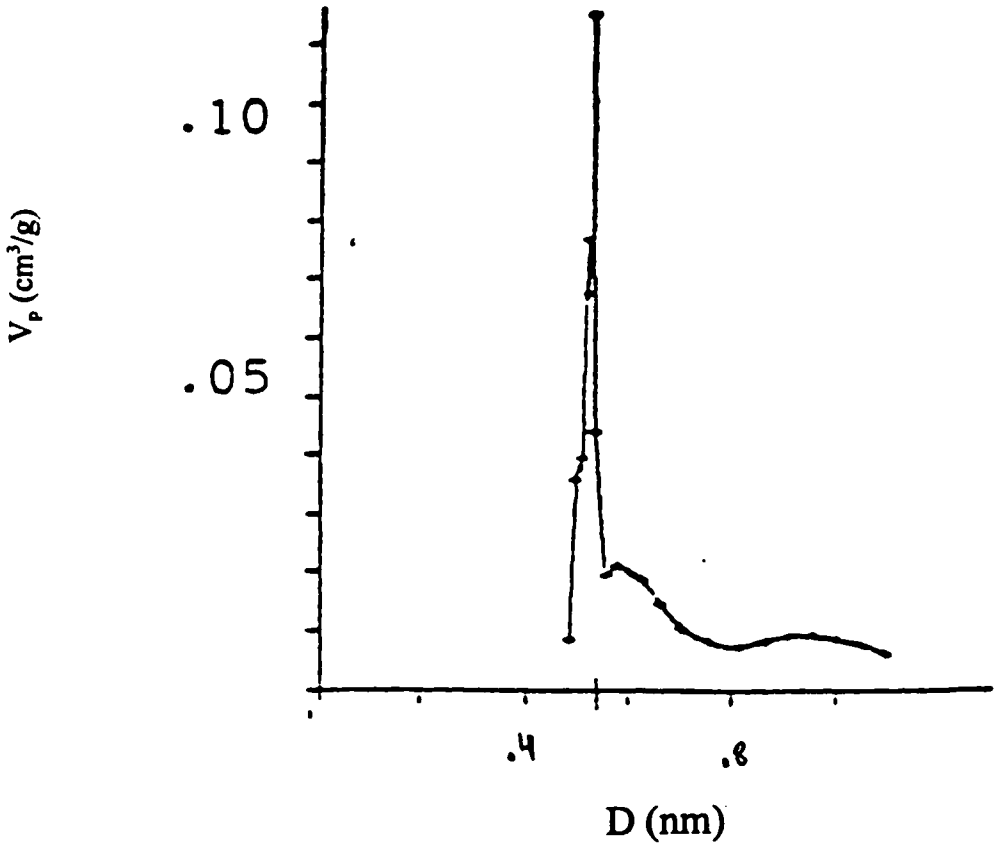

Figure 4.6 Micropore Size Distribution of the Parent Sample Activated at 550 °C Overnight .

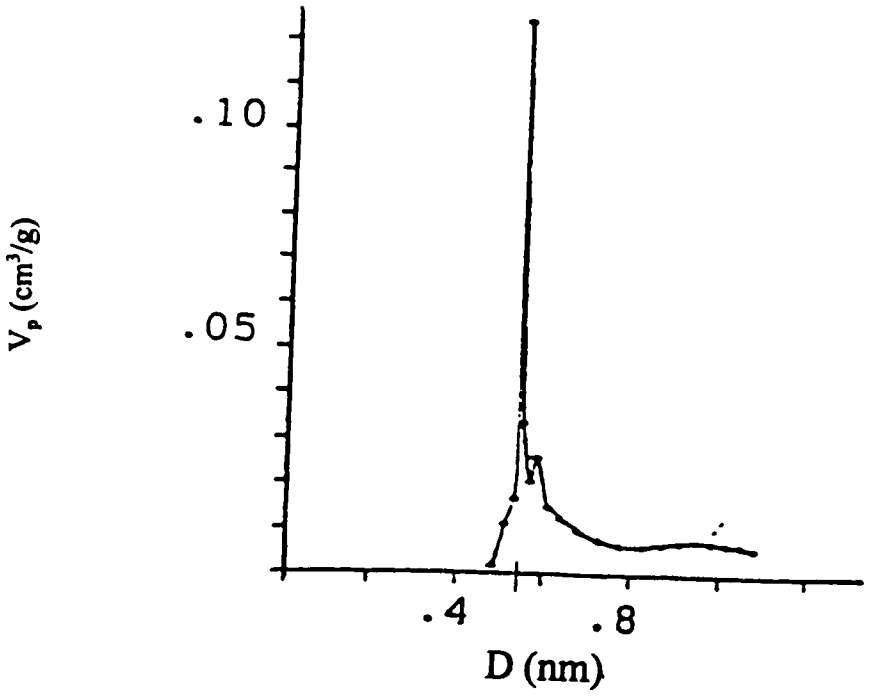

Figure 4.7 The Micropore Size Distribution of the Desilicated (NaDZSM-5) activated at 550 ^{0}C Overnight .

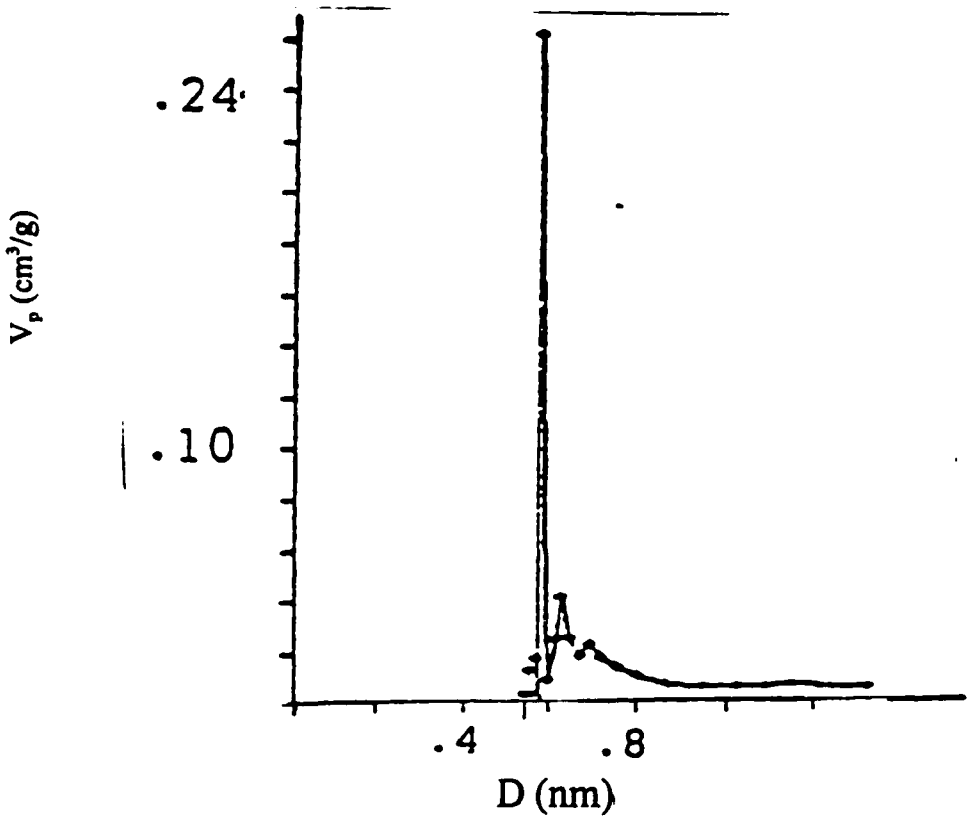

Figure 4.8 Micropore Size Distribution of the NaDZSM-5 (2.5) activated at 550 ^{0}C overnight .

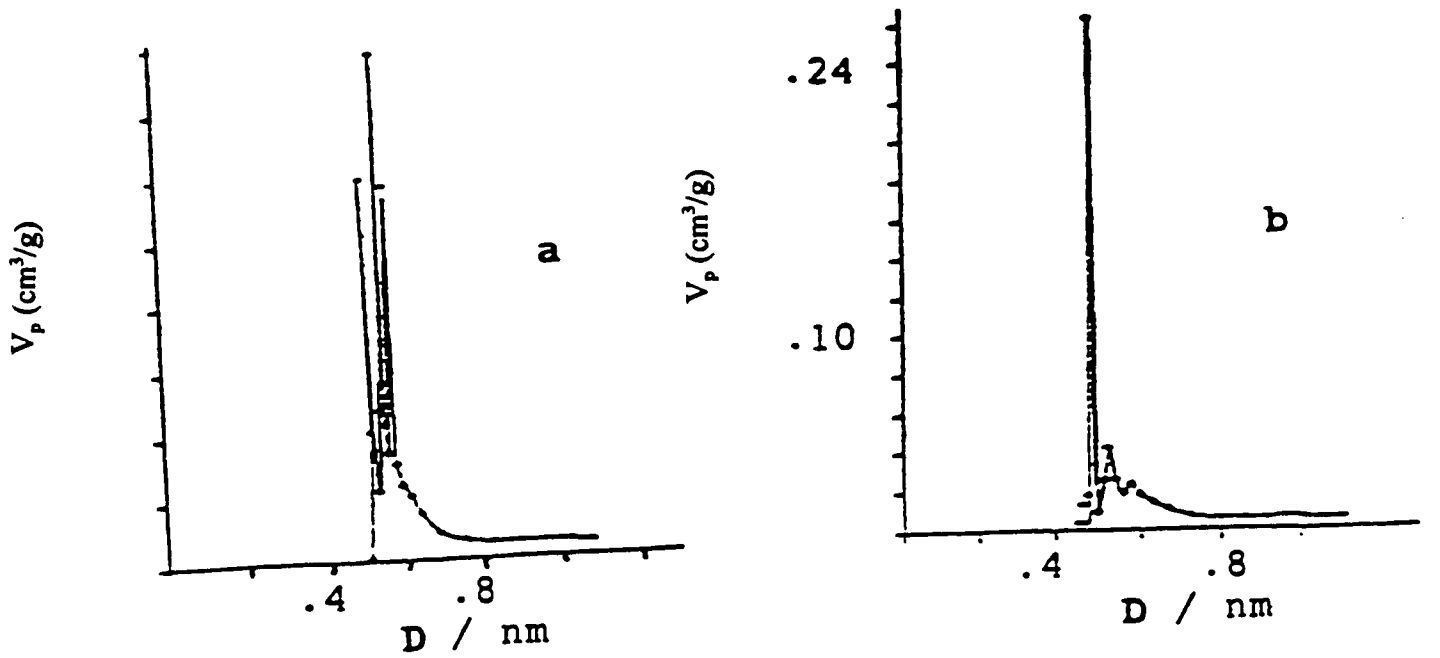

Figure 4.9 Stabilization of the NaDZSM-5 (2.5) Sample a) heated 220 ^{0}C and b)heated at 550 ^{0}C .

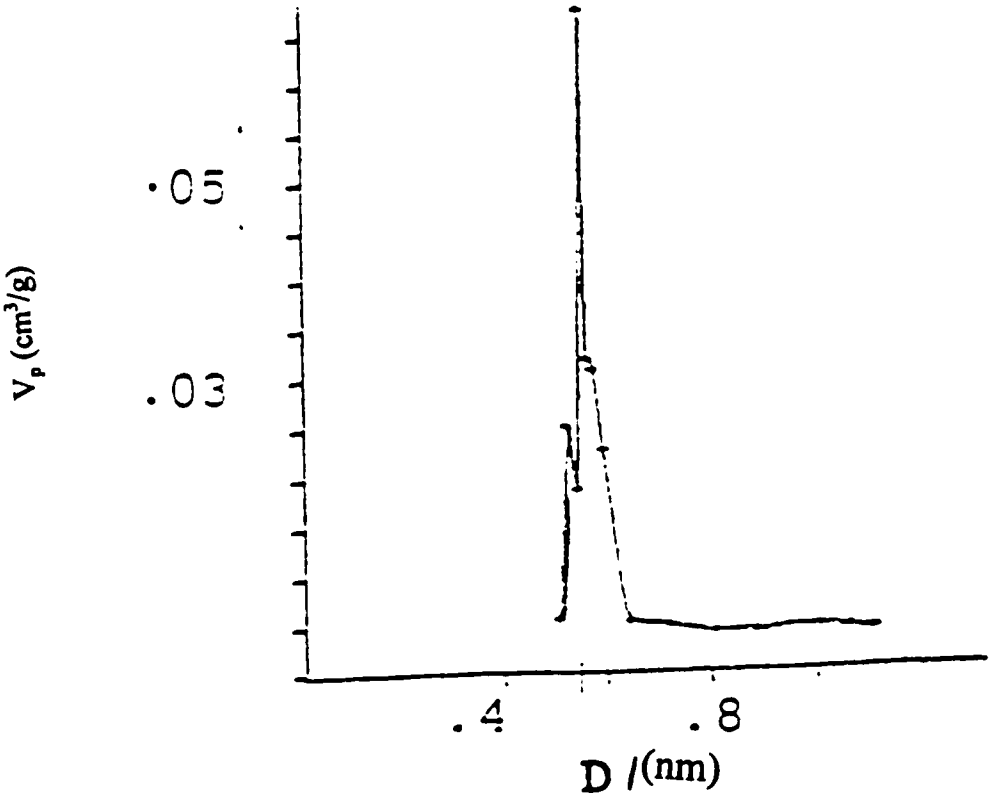

Figure 4.10 Micropore Size Distribution of the NaDZSM-5 (5.0) activated overnight at 550 ^{0}C .

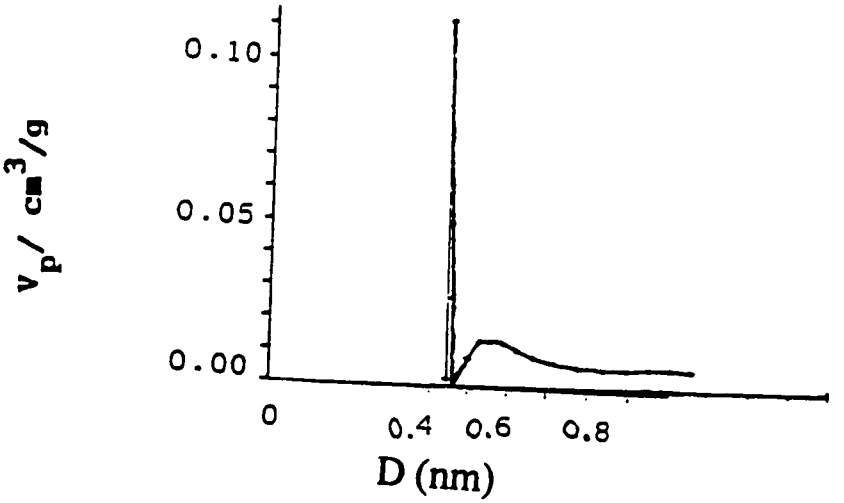

Figure 4.11 Micropore Size Distribution of the desilicated sample (NaDZSM-5) heated at 220 ^{0}C overnight .

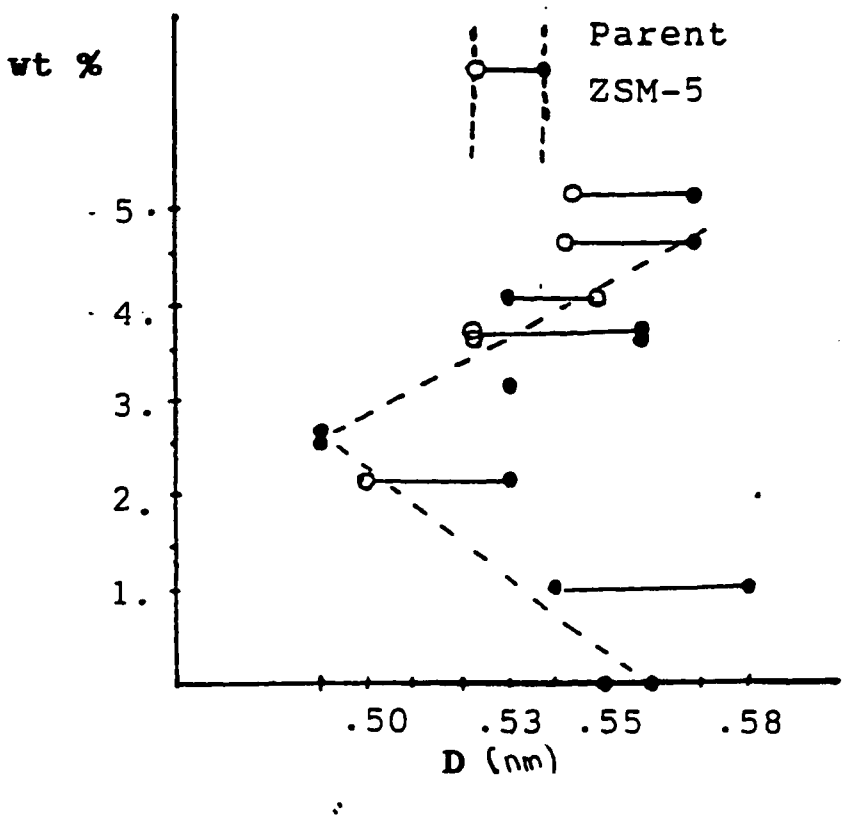

Figure 4.12 Variation of the Micropore Size Distribution with (Si-O) species loading into the desilicated zeolite versus the Diameter (nanometers) , where the full dots indicate the most intense peak(s) in the distribution curve .

The results obtained from the surface area measurements gave a good indication that the structure has not changed drastically compared to the parent .It is know that what was extracted contained mostly sodium orthosilicate and its dimer sodium pyrosilicate , but the analysis of the sample showed that trace amounts of sodium metasilicate were present .Experiments were then performed to analyze 4 samples (see fig. 4.5) all activated at 550 ^{0}C , using X-ray powder diffraction .The peaks that could be influenced were in the region of 2θ $(22.5\text{-}25.0)^0$ .The parent was given the value of 100 % regarding the crystallinity. Even though the value for the crystallinity of the desilicated and the 2.5% ortho were lower than the parent , one could say that the structures did not change during the desilication / reinsertion treatments . As for the metasilicate sample , it could be said that even though it is still in the 80 % ,range which could be acceptable , the fact is that it is much lower than the value for the orthosilicate . We therefore have to consider that adding 2.5 % metasilicate changes the structure in a certain way , so as to give a value much different than after addition of 2.5% (Si-O) species .

Table 4.19 Wavenumber (cm^{-1}) of some FT-IR bands in the Framework Region and ^{29}Si MAS-NMR area ratio R [= Si (1 Al) / Si (0 Al) , obtained by the method of peak deconvolution] .

Sample	Si/Al ratio (Δ=0.1%)	DC (%) (Δ=3%)	ν asym. (cm^{-1})	ν sym. (cm^{-1})	R
Parent ZSM-5	23.3	100	1127	796	0.163
DZSM-5	17.1	89	1101	798	0.225
DZSM-5 (2.5)	17.4	86	1107	797	0.207

The above table ,shows that the Si/Al ratio decreases from the parent to the desilicated sample as expected, and that adding Si-O species helps it go back up .

As reported earlier , the x-ray powder diffraction instrument allowed to determine how close the 3 samples were to each other structure wise .The results showed that the structure did not change during the desilication / reinsertion treatment although the crystallinity degree (DC) of the two modified zeolites were a little lower than that of the parent zeolite .

The FT-IR results were separated into 2 types : 1) the asymmetric stretching band is defined as being structure insensitive which means that it is dependant on the Si/Al ratio .In our case we see that as the Si/Al ratio decreases, there is a decrease in the value of the stretching band, which is assigned to the framework T-O-T bonds, and any shift to a higher frequency resulted from an increase in the framework Si/Al ratio . 2) The symmetric stretching band is structure sensitive, which means that if the zeolite structure changes we are going to have a change in the value. No such change was observed for our 3 samples .

The ^{29}Si MAS-NMR spectrum of the parent ZSM-5 showed two peaks with the most intense one at -113 ppm (see fig.4.13) being assigned to Si(0Al) . This indicates that it had no aluminum neighbors and the shoulder peak is assigned to the Si(1Al) . After desilication the R value (area ratio) increased because desilication increases the amount of neighbor aluminum around the central silicon. This indicates that there was actual removal of silicon from the framework during desilication without modification of the aluminum tetrahedral sites . As expected resilication brought about a decrease of the R ratio back to a value closer to the parent zeolite because silicons are regaining their positions around the central .

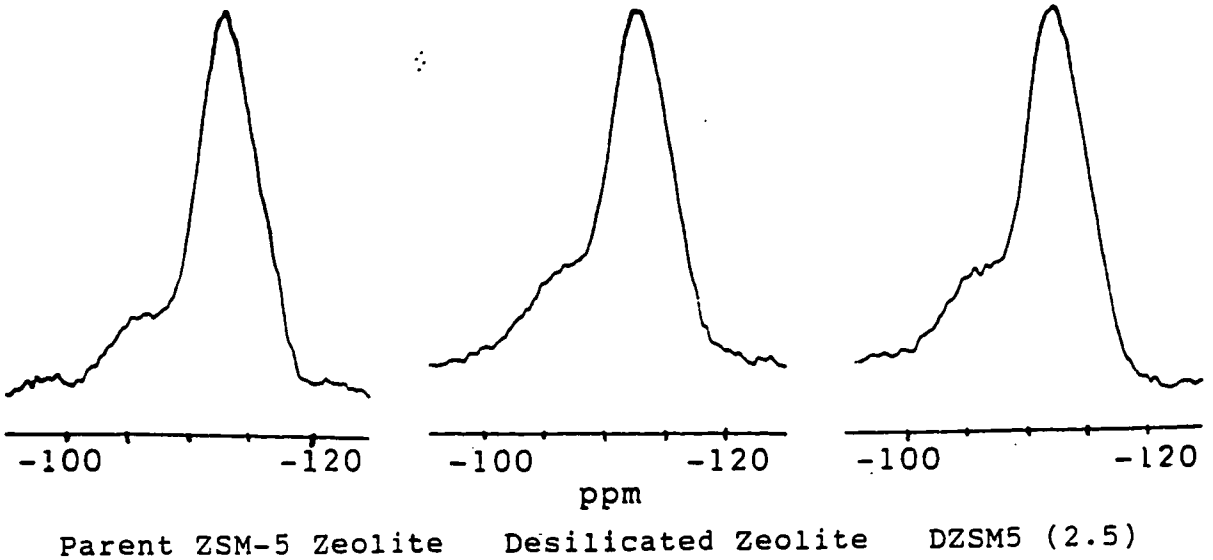

Figure 4.13 ^{29}Si MAS-NMR of : a) ZSM-5 ; b) DZSM-5 and c) DZSM-5 (2.5)

Chapter 5

5.1 Conclusion

By using the DRS procedure which stands for desilication , resilication and framework stabilization , we were able to prepare a sodium form ZSM-5 with very specific characteristics which are : 1) having the same structure as the parent ZSM-5 zeolite and 2) uniform micropores whose size may be varied by + or - 0.4 Å with respect to the average size of the original micropores .The key factors which are at the basis of the DRS method are : i) the extent of the desilication , ii) stabilization mechanism which is still unknown and iii) the migration of the reinserted silicon layer during the thermal treatment leading to framework stabilization .Such zeolites have novel microporosities and high thermal stability . This process will have very interesting applications in catalysis for shape selectivity and possibly in other fields such as selective adsorption / separation or even ion-exchange . Preliminary tests were made on the ammonium form ZSM-5 and we could see that the same type of results as with the sodium form ZSM-5 were achieved , showing that the process is expandable to other cationic forms of the ZSM-5 zeolite .

The results showed unequivocally that with the sodium form zeolite, the removal of calcium and magnesium ions was improved by performing desilication and then heating the treated samples to higher temperatures . For samples heated from 350 ^{0}C to 550 ^{0}C a variation of 70 % compared to the parent samples heated from 110 ^{0}C to 450 ^{0}C was observed. We also performed the same tests with X (7.4 Å) and Y (7.4 Å) zeolites comparing the values to Na-A (4.2 Å) .Results show that at ambient temperature the removal was the greatest for the Na-A zeolite .

It may be practical to try and use the DRS method on other types of zeolites that have a special type of microporosities and are thermally very stable such as the X and Y zeolite . To improve the selectivity by increasing or decreasing the size of the pores for such applications as : catalysis , adsorption/separation very useful in ultrafiltration , reverse osmosis and gas separation , one should use the DRS method . To improve the ion-exchange, one needs to decrease the Si/Al ratio , which increases the concentration of aluminum , and the size of the pores while favoring better diffusion. In the case of the acid form ZSM-5 , this method may have some important applications in the FCC process in shifting the production to get more ethylene / propylene with a zeolite pore size of 4.9 Å or to maybe shift

towards isobutene / Isoolefins with a pore size of 5.5 Å or higher .The latter FCC products may have some important implications for the synthesis of gasoline octane enhancers such as MTBE or TAME , which use them as feedstocks .

5.2 Future Work

We have been able to develop the method of DRS with zeolites that have a Si/Al ratio of 23 and 40 . The important aspect of this Masters thesis was to find out if this method would work , what characteristics this would give to our zeolite material and lastly if we would be able to reproduce it on a regular basis so it may be produced and used by industry .

Once that we know that our process works well for these zeolites , we wanted to know if this would work for silicalite which has a Si/Al ratio of more than 150 . The desilication step tends to influence the production of "desilication" "holes"or Si vacancies . The next important point that we would need to find out is the reaction mechanism that would explain the reinsertion of the Si-O species back into the framework . Another question that would have to be answered is if the Si/Al ratio of a zeolite plays a role in the reaction mechanism . It may be that a change in the ratio brings about a change in the amount of Si-O species which needs to be added to get a specific pore size either narrower or larger on the dimension's scale .

We have seen that performing desilication of up to 30 % gave the results seen in this thesis . If we perform desilication of smaller amount , for example 5% , 10% , 15% .... would this give us the same effect or not ? If we

would not have the same effect then how low may I go for desilication and still get the same results.

We have found that sodium orthosilicate works well , but it contains also the dimer sodium pyrosilicate and smaller quantities of metasilicate . It would be interesting to try adding only sodium metasilicate and attempt to see if we could find the right conditions to make the reinsertion work . Maybe once we find those conditions , this may work even better than with the sodium orthosilicate / sodium pyrosilicate species . We have to test the samples with the following measurements : Pore size distribution , NMR ^{29}Si and FT-IR to help us follow the silicon species which has been reinserted .

More extensive testing needs to be done to see if the re-incorporation disturbs the aluminum sites in anyway because if it does then this would decrease the effectiveness of our newly synthesized material to work well in the ion-exchange capacity (shape selectivity) .As we have seen , the role of the acid sites is of the uttermost importance to us and we could test them by using ion-exchange capacity of the calcium and magnesium ions .

In conclusion the following steps are needed to be help us understands fully what is going on within this DRS process .We need to find the reinsertion mechanism and understand it totally . Direct Observation (ion-

exchange) and indirect observations (Catalytic activity) need to be done to see if any changes have affected the aluminum sites . We need to find out what is the effect that water has on the stabilization process (steam treatment) at low temperatures .We have to try out these samples in a very important process which is the methanol to gasoline process (MTG) . In this process , the zeolite shape selectivity is a key parameter for the product spectrum .A pore size of 4.9Å gives us light olefins and light hydrocarbons , a pore size of 5.6 Å gives us premium gasoline and lastly a 5.7 Å pore size gives us kerosene . So depending on what we want to produce and a given time , we just have to change the catalyst to change the product we want .[76]

Appendix

AP.1 Atomic Absorption Spectrophotometry

A.1.1 Theory

Atomic absorption spectroscopy (AAS) was used for elemental analysis of Al , Na and Si which is expressed as SiO_2 was obtained by subtracting the sum of the Al_2O_3 and Na_2O percentages from 100 . Since the relative quantities of each of these elements will directly affect the catalytic and adsorptive properties of the molecular sieves . We could classify zeolites according to the ratio of Si/Al tetrahedra in their framework .

AAS is based on the principle that metal atoms absorb electromagnetic radiations at frequencies which are characteristic of each metal , and the amount of light absorbed is a function of the metal concentration . This is one of the most used analytical tools in modern analytical laboratory , mainly by the use of the hollow-cathode discharge lamp as a light source and the use of atomizers to provide rapid and efficient atomization of liquid samples . With current instrumentation , however the method is not suitable for qualitative or simultaneous multi-element analysis [80] .

Qualitative analysis by AAS is based on the measurement of the

radiant energy absorbed by free atoms in their gaseous state . Because the spectra of gaseous atomic species consist of well-defined narrow lines at a wavelength characteristic of the element involved , it is known to be a high selectivity technique. The solution samples are vaporized , commonly by flames , electrical heating or lasers ; and on further heating the vapor dissociates into free atoms . From figure 3.4 , we could see a schematic presentation of this process .

Since the element of interest does not usually exist as free atoms in any common solution but is in the ionic state or in a molecular form , it is necessary to generate a population of free neutral atoms of the element of interest in order to observe AA signals . The metal atoms are then capable of strongly absorbing radiations at discrete characteristic wavelength , which coincide with the narrow emission lines of the particular metal generally provided by a hollow cathode lamp . Hence , the theory of AA concerns the formation of free atoms from the sample , which are in an unexcited ground-state level and this absorption of radiation [81] .

Because most of the atoms remain in the ground-state , absorption is greatest for resonance lines resulting from transitions originating from the ground-state and this therefore , greatly restricts the number of absorption

lines that can be used in atomic absorption . The degree of absorption depends on the population of atoms in the ground-state and the ability of these absorbing atoms . Such a degree of absorption is an expression of the line intensity and represents the probability that an atom will undergo a transition per unit time .

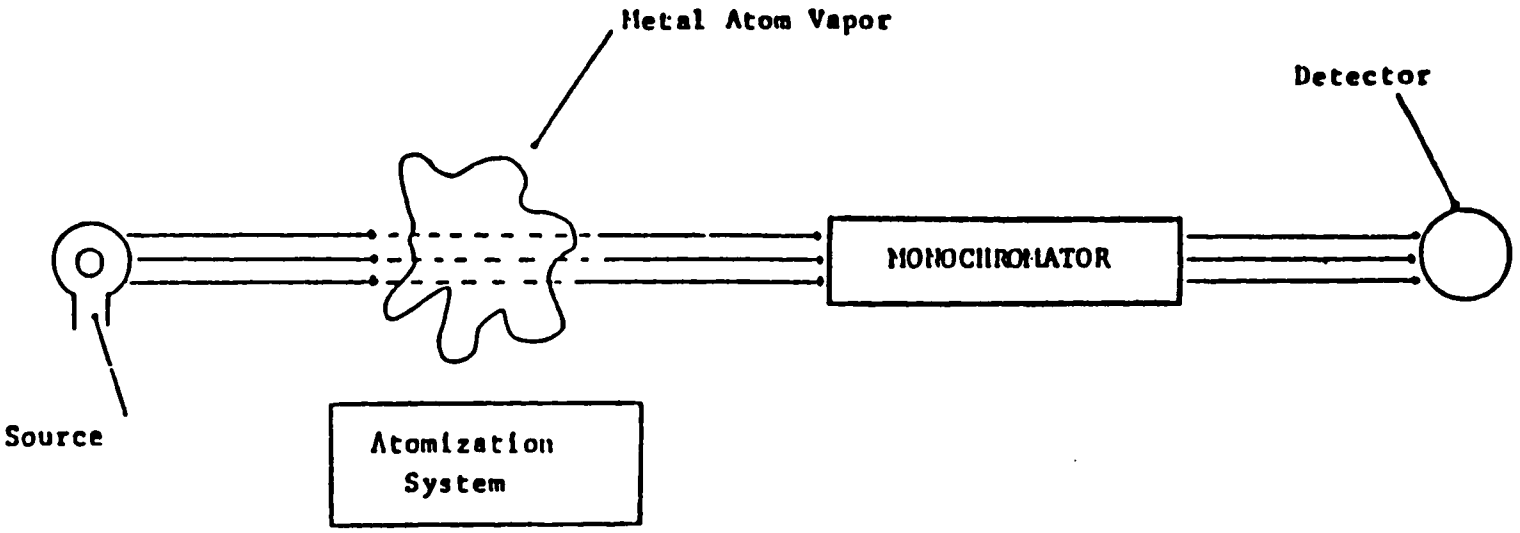

Figure A.P 1. A Schematic Presentation Of the Concept Of Atomic Absorption Spectroscopy .

The degree of absorption is a function of the concentration of the metal in the sample while the absorption follows Beer's Law where the absorbance is directly proportional to the path length in the flame . Both of these variables are difficult to determine . However , the path length can be held constant and the concentration of the atomic vapor is directly proportional to the concentration of the analyte in the solution being aspirated [82,83] .

Similarly to Lambert's law , we have :

$$I = I_0 \exp(-K_v B)$$

where : I = intensity transmitted by the sample

I_0 = incident beam

K_v = absorption coefficient characterizing the intensity

B = horizontal path length of the flame or thermal source

Since the physical property actually is measured in absorbance A , we then have : $A = \log (I_0/I) = K_v \log e = 0.4343\ KvB$

The absorbance is directly proportional to the absorption

coefficient K_v which is directly proportional to the number of absorbing atoms and therefore to the concentration of the solution . Thus , plots of absorbance at the specified wavelength against concentration should yield a linear relationship .

A.1.2 Instrumentation

There are two parts with essentially different functions : the means whereby the population of ground-state atoms is produced from the sample and the optical system . The basic components of an AA spectrometer include : A) A radiation source to emit the spectral line of the element of interest .

B) An atomization system (flame or furnace) to provide sufficient energy for analyte dissociation and vaporization as free atoms .

C) A monochromator for spectral dispersion and isolation of the spectral lines to be measured .

D) A detector and data - logging device to measure , amplify and display the results.

The most critical component of an AA spectrophotometer is the source.

The hollow cathode lamps which have been used almost exclusively as the radiation source for most elements ,emits strong sharp lines of appropriate wavelength characteristic of the desired element .This radiation then passes through a flame into which the sample solution is sprayed as a fine mist . Under the experimental conditions , the predominant ground-state atoms , thermally generated by the flame , absorb the resonance radiation from the source lamp and reducing hence the intensity of the incident beam [81] .

The monochromator and the slits isolate the desired resonance line from other radiations emitted by the source and allow it to fall in the photo multiplier detector which then converts the light signal into an electrical one . Since the range of wavelengths detected is determined primarily by the hollow-cathode source , the monochromator and slits serve primarily to minimize the detected background radiation from the flame and also to remove extraneous lines emitted by the hollow cathode filler gas . The emitted radiation corresponding in wavelength to the monochromator setting is inevitably present in the flame , due to excitation and emission by the analyte atoms . The thermally excited emission by the analyte atoms is therefore discriminated by modulating the source of radiation and using an

AC amplifier : the unmodulated emission is not detected . The signals generated by the photoelectric detector are amplified by an amplifier tuned to the frequency of modulation while the radiation emitted by the flame is not modulated , and gives therefore no resulting output signal [84].

Since reducing the sample to the free atomic state , it is necessary to achieve absorption by atoms , the most common atomization device spectroscopy consists of a nebulizer and a burner [85] . The nebulizer converts a sample solution into a fine spray or aerosol which is then fed into the flame. The analyte solution is first aspirated from the sample container through a capillary tube by suction (Venturi action) caused by rapid flow of support gas (oxidant) past the capillary tip . The resulting aerosol is then mixed with the fuel and flows past a series of baffles which remove all but the finest droplets.

The flame evaporates the solvent , decomposes and dissociates the molecules into the ground-state atoms . Its use as the atom cell in analytical AA is at present , by far the most widely used method to obtain a population of free analyte atoms .

A.1.3 Atomic Absorption Analysis

A Perkin-Elmer model 503 AA spectrophotometer utilizing a double-beam optical system and a Perkin-Elmer 56 digital recorder were used . The dispersion optical system included also a high quality diffraction grating monochromator .

A laminar flow (Premix) burner was used , equipped with two single-slot burner heads : a 10-cm long for air-acetylene and 5-cm long for nitrous oxide -acetylene , respectively . The burner heads were held in place by stainless steel cables and a safety pin interlock [86] .

A.P.2 X-Ray Powder Diffraction (XRD)

A.2.1 Theory

X-ray diffraction is a very powerful technique , it is used for phase identification , quantitative phase analysis , structure determination and the study of the crystallinity of solids . Knowing that zeolites are crystalline micropores solids whose catalytic properties , such as unique shape selectivity , homogeneity and porosity , depend on their structural integrity and crystallinity , so it is important that zeolites exist in a form in which they possess their highest crystallinity ,chiefly for the purpose of exercising their maximum advantages in shape selective catalytic reactions [87] .

We could define a crystal type in terms of the lengths of the sides of its smallest repeating structure which is called a unit cell . The regular repetition of the unit cell gives rise to planes throughout the crystal and so each crystal structure is characterized by a very unique set of families of parallel planes at different orientations . The d-spacing is the distance between 2 adjacent planes of a given family (fig. Ap.2) . So each crystalline material is characterized by a unique set of d-spacings . Since the wavelengths of x-rays are of the same order of magnitude as the interplanar spacings and can be constructively scattered from them to give a diffraction pattern , a unique x-

ray pattern for each crystalline material can be obtained which allows for the identification of the crystalline materials [87] .

An x-ray beam incident on a crystal will be diffracted by the regularly repeating array of scattering centers which are electron clouds surrounding the atomic nuclei in the crystal . As shown from figures Ap.3 and Ap.4 , the angle throughout which the x-ray diffracts depends upon the spacing between the planes of the atoms in the crystal . Hence Bragg's equation was derived as follows :

$$N\lambda = 2d \sin \theta \quad (15)$$

where : N = an integer , expressing the order of diffraction

λ = x-ray wavelength

θ = angle of diffraction

d = interplanar spacing

One of the methods which is the most frequently used for phase identification is the powder method . The single crystal diffraction method is much better suited for crystal structure determination .

We could get a diffraction pattern of all possible planes , if a monochromatic beam of x-rays strikes a fine homogeneous powder , which is formed from an enormous number of small crystallites randomly oriented in every possible direction . What is expected is that a certain number are oriented in such a way that Bragg's condition for diffraction is fulfilled from every possible interplanar spacing .

The main objective of an x-ray powder diffractometer is to measure the intensity of the diffracted x-rays as a function of the angle θ between the incident beam and the surface of the sample . The θ angle is called the Bragg angle and typically instruments give the intensity of x-rays versus 2θ . The 2θ values which are the angles between the incident beam and the diffracted beam can be converted to d-spacings using Bragg's relation [80] .

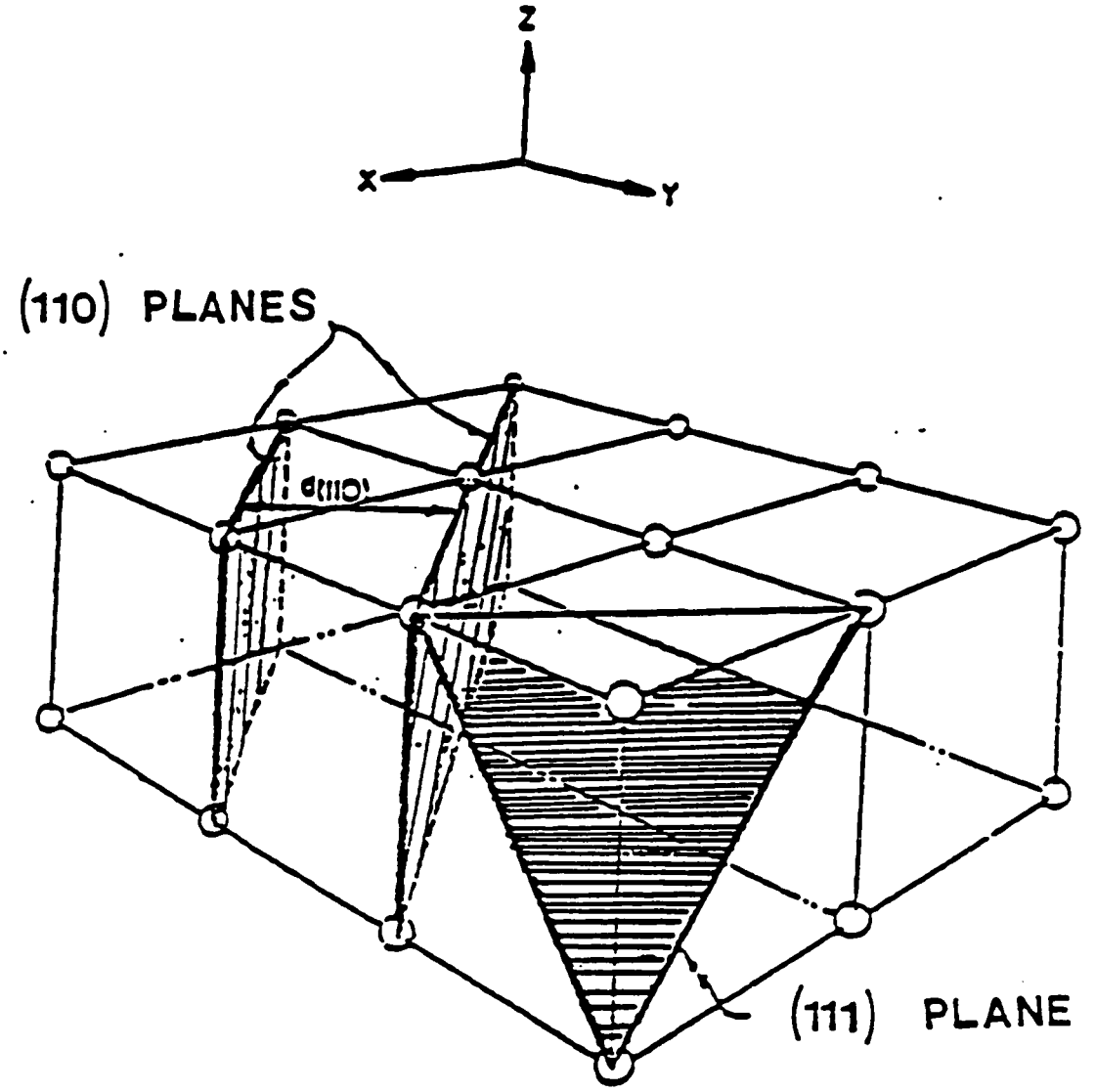

Figure Ap.2 Representation of A Simple Cubic Crystal Structure Showing Atoms , two adjacent (110) planes and the interplanar Spacings d(110) between them .

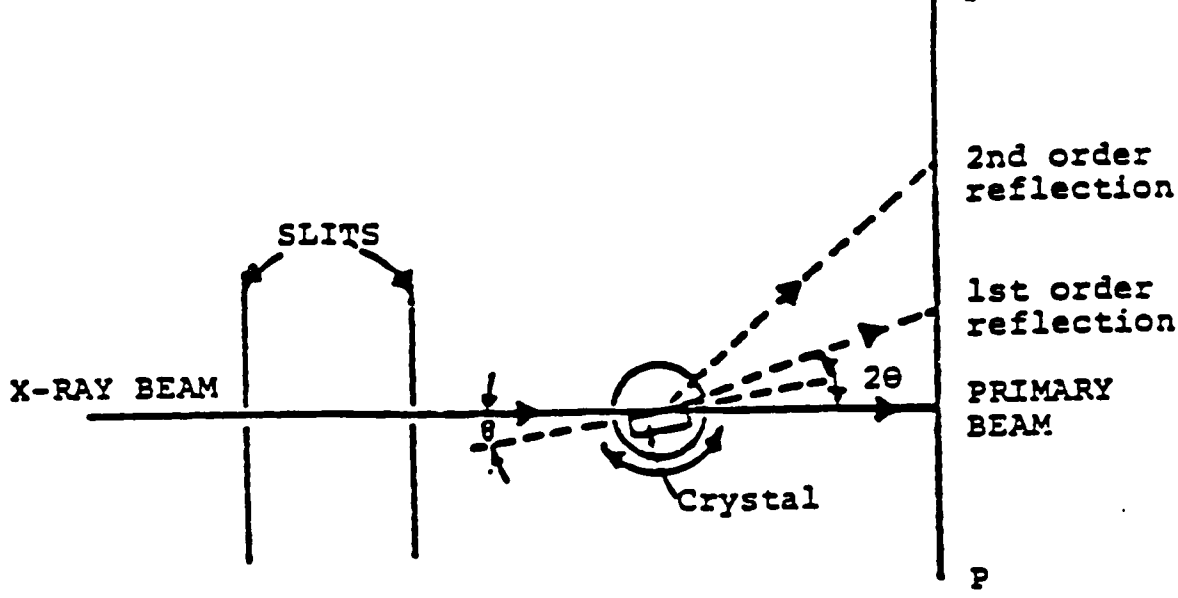

Figure Ap.3 Diffraction of Radiation from a Crystal .

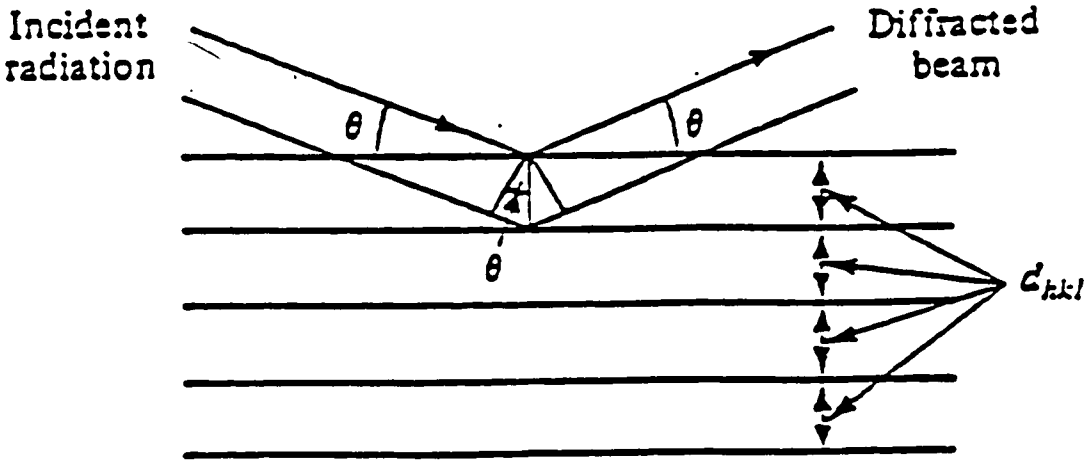

Crystal planes (h, k, l)

Bragg condition: $n\lambda = 2d_{hkl} \sin \theta$

Figure Ap.4 Reflexion Analogy of X-Ray Diffraction .

A.2.2 XRD Analysis

We used a Philips PW 1050/25 automated X-ray powder diffractometer which was powered by a Philips x-ray generator line focusing goniometer and a scintillation counter . The measurements were done using a Philips long fine focus copper x-ray tube . Copper K_{α} monochromatic radiation with λ = 1.5418 Å was obtained by using a nickel filter . The data acquisition was carried out using the step scanning mode and was computer controlled using the Sie 112 software from Sietronics . Peak determination and background removal was all done using the Sie 112 software [88] .

REFERENCES

1. D.Breck , Zeolite Molecular Sieve - Structure , Chemistry and Use , J.Wiley and Sons , N-Y , 147 (1974) .

2. E.F Vansant ,"Pore Size Engineering in Zeolites" , Wiley and Sons , 8 ,113 (1990) .

3. R. Le Van Mao , G. Denes , N.T.C Vo , J.A. Lavigne and S.T Le , "Production of Porous Materials by Dealumination of alumina- rich zeolites ", in Advances Porous Materials Research Society Symposium, **371** , 125, (1995).

4. Lucio Forni , "Standard Reaction Tests For Microporous Catalysts Characterization" , Catalysis Today , **41**, 223, (1998) .

5. Bruce C. Gates , Catalytic Chemistry , Wiley and Sons , USA , 397 (1992) .

6. A. Ramsaran , "Desilicated ZSM-5 Zeolite As Catalyst For The Dehydration of Ethanol", Ph.D Thesis ,Concordia University, 12 (1996) .

7. J. Yao , "Aromatization Of Short Chain Alkenes Over Gallium Modified ZSM-5 Catalysts , Ph.D Thesis ,Concordia University, 7 (1992) .

8. J.T. Richardson , "Principles of Catalyst Development" , Plenum Press , New-York and London , 77 (1989) .

9. L. Louis Hegedus , Alexis T. Bell , N.Y. Chen , Werner O.Haag et al. , "Catalysis design , Progress and Perspectives" , A Wiley-Inter -Science Publ., John Wiley and Sons , 114 (1987) .

10. D.E.W. Vaughn , Chemical Engeneering Progress , 25 (Feb. 1988) .

11. W.A Haag , "Zeolites and Related Microporous Materials" ; State of the Art Studies in Surface Science Catalysis , **84** , 1375 (1994) .

12. R.J. Farrauto , R.M. Heck and B.K. Speronello , Hydrocarbon Processes, **71** , 31 (1992) .

13. M. Iwamoto ,"Zeolites and related Microporous materials":State of the art Studies in Surface Science Catalysis , **84** , 1395 (1994) .

14. A.T. Bell , Chemical Eng. Progress , 26 (Feb. 1995) .

15.S.Ainsworth , Chemistry and Engineering , 34 (Jan. 1994) .

16. J. Armor , Chemtech , 557 (Sept. 1992) .

17. M.E. Davis , Industrial Engineering Chemical Resources , **30** , 1675 (1991) .

18. Z. Li , C.Lai and T.E. Mallouk , Inorganic Chemistry , **28** , 178 (1989) .

19. S.M. Scicsery , Zeolites , **4** , 202 (July 1984) .

20 . R. Morrison and R. Boyd ,Organic Chemistry 3rd Edition , Allyn and Bacon inc., 32-34 (1979) .

21. C.N. Satterfield ," Heterogeneous Catalysis in Industrial Practice" , McGraw- Hill, 202-210 (1991) .

22. R. Le Van Mao , S. Xiao and T.S.Le ,"Thermal Stability of The Pt Bearing Superacidic Sulfate-Promoted Zirconia in the presence of Hydrogen ", Catalysis Letters , **35** , 107-108 (1995) .

23. R. Le Van Mao , S. Xiao , J.Yao and A. Ramsaran ,"Selective Removal Of Silicon from Zeolite Frameworks Using Sodium Carbonate ", J. Materials Chemistry , **4** (4) , 605 (1995) .

24. C.N. Satterfield ," Heterogeneous Catalysis in Industrial Practice" , McGraw- Hill, 171-173 (1991) .

25. N.Y Chen , W.E Garwood and F.G Dwyer , Shape Selective Catalysis in Industrial Applications ,Marcel Dekker inc., 26-27 (1989) .

26. Morrison and Boyd 3rd Edition , Organic Chemistry , Allyn and Bacon inc. 40-41 (1979) .

27. E.Brunner , K.Breck , M.Koch , H. Pfeifer , B. Staudte and D. Zscherpel , "Zeolites and related Microporous materials" : State of the art Studies of Surface Science Catalysis , **84** , 357 (1994) .

28. A. Ramsaran , "Desilicated ZSM-5 Zeolite As Catalyst For The Dehydration of Ethanol", Ph.D Thesis ,Concordia University, 26 (1996) .

29. H.Pfeifer , D. Freude and M. Hunger , Zeolites , **5** , 274 (Sept 1995) .

30. J.Scherzer , Octane Enhancing Zeolite FCC catalysts , Marcel Dekkar inc. , 44 (1990) .

31. A. Ramsaran , "Desilicated ZSM-5 Zeolite As Catalyst For The Dehydration of Ethanol", Ph.D Thesis ,Concordia University, 28-29 (1996) .

32. D. Barthomeuf , Zeolites **14** , 394 (July - August 1994) .

33. Bruce C. Gates , Catalytic Chemistry , Wiley and Sons , USA , 470 (1992) .

34. P.Batamack , C.Dormieux Morin , R. Vincent and J. Fraissard , Journal of Physical Chemistry , **97** , 9779 (1993) .

35. W. Loweinstein , American Mineral ., **39** , 92 (1994) .

36.A. Ramsaran , "Desilicated ZSM-5 Zeolite As Catalyst For The Dehydration of Ethanol", Ph.D Thesis ,Concordia University, 53-54 (1996) .

37. D.Breck , Zeolite Molecular Sieve - Structure , Chemistry and Use , J.Wiley and Sons , N-Y , 261 (1974) .

38. J.R. Goldsmith , Journal of Geology , **61** , 439 (1953) .

39. Bruce C. Gates , Catalytic Chemistry , Wiley and Sons , USA , 287 (1992) .

40.Bruce C.Gates , Catalytic Chemistry , Wiley and Sons , USA , 269-270 (1992) .

41. D.H Olson , W.O Hoag and R.M Lago , Journal of Catalysis , **61** , 390 (1980) .

42 . W.A. Haag ," Zeolites and related Microporous Materials" ; State of the art Studies in Surface Science Catalysis , **84** , 1375 (1994) .

43. D. Barthomeuf , Zeolites , **14** , 396 , July/August (1994) .

44. H.Pfeifer , J. Chem. Soc. Faraday Trans. 1 , **84** , 3777 (1988) .

45. C.N. Satterfield , Heterogeneous Catalysis in Industrial practice , Mcgraw Hill , 230-231 (1991) .

46. Israel E. Wachs , Characterization of Catalytic Materials , Manning Publ. , 135 (1992) .

47 . R.M. Dessau , E.W. Valyocsik and N.H. Goeke , Zeolites , **12** , 776 (1992)

48. G. Lietz , K.H. Schnabel , G. Peuker , W.Storck and J.Volter , Journal of Catalysis , 562 (1994) .

49. R.Le Van Mao , A. Ramsaran , S. Xiao and J. Yao , "pH of the Sodium Carbonate Solution Used for the Desilication Of Zeolite Materials ", J. Materials Chemistry 5(3) , 533 (1995) .

50. R. Le Van Mao , S. Xiao , A. Ramsaran and J. Yao , " Selective Removal of Silicon from the Zeolite Framework using Sodium Carbonate ", J. Materials Chemistry 4(4), 609-610 (1994) .

51. D.W Breck , Potential uses of Natural and Synthetic Zeolites in industry , Union carbide Corporation Brochure , 25 (1979) .

52.. G.Horvath and K. Kowazoe , J. Chemical Engineering in Japan **16**(6) , 470 (1983) .

53. R. Le Van Mao , N.T. Vu , S.Xiao and A. Ramsaran ," Modified Zeolites For the Removal of Calcium and Magnesium from Hard Water "
J. Materials Chemistry ,4(7),1143 (1994) .

54. G.Engelhardt and D.Michel , "Solid State NMR of Silicates and Zeolites " ,
John Wiley and sons , 157-161 (1987).

55. B.H Davis , Chemtech , 19 (Jan 1991) .

56. B. Shapiro , "Heterogeneous Catalysis " , ACS symp. , **288** , 349 (1984) .

57. A.J Lecloux , B. Anderson and S. Boudant , " Catalysis : Science and Technology " , ed. Springer-Verlag , Berlin , **2** ,183-185 (1981) .

58. S.J. Gregg and K.S King " Adsorption Surface Area and Porosity " Academic Press inc. , London , 140 (1982) .

59.R. Le Van Mao , S.T. Le , D. Ohayon , F.Caillibot ,L. Gelebart and G. Denes ; " Modification of the Micropore Characteristics of the Desilicated ZSM-5 Zeolite by Thermal Treatment " , Zeolites **19** (4) , 277 (1997) .

60. G.Horvath and K. Kowazoe , J. Chemical Engineering in Japan **16**(6) , 474 (1983) .

61. Operator's Manual of Micrometrics - ASAP 2000 Operating Programs V.1.03, Norcross , Ga (1993) .

62. D. Freude , "Studies of Surface Science Catalysis " , **52** , 169 (1989) .

63.D.Breck , Zeolite Molecular Sieves : Structure , Chemistry and use , J. Wiley and Sons , N-Y , 249 , 514 (1974) .

64.R. Le Van Mao and D.Ohayon , " Thermally Stable ZSM-5 Zeolite Materials With New Microporosities ,Proc. 12th International Zeolite Conference , Baltimore , USA (July 1998) in Press .

65. L.R Morris , "Spectrochem . Acta" , **35B** , 687 (1980) .

66 .P.K. Kipkemboi , " Preparation and Characterization of Leached Asbestos Materials " , MSc. Thesis , Concordia University , 177 (1988) .

67.G.W Skeels and D.W Breck , , Proceedings of the 6th International Zeolite Conference , Butterworth -Heinemann , Stoneham ,Ma. , 87 (1984) .

68.S.B Kulkarni ,V.P. Shiralkar , A.N. Kotasthane , R.B. Borade , and P.Ratnasamy , Zeolites , **2** , 313 (1982) .

69. Dai F.Y Suzuki , M. Takahashi , Hand Saito , Zeolite Synthesis ACS Symp. Sec. 398 , American Chemical Society , Washington , D.C , 244 (1989)

70 .V.R. Choudhary and V.S. Nayak , Zeolites , **5** , 325 (Sept. 1985) .

71. C.D. Chang , C.W. Chu and R. Socha , J. of Catalysis , **86** , 289 (1984) .

72. R. Le Van Mao , N.T. Vu , S. Xiao and A. Ramsaran ," Modified Zeolites Removal of Calcium and Magnesium from Hard Water " , J. Materials Chemistry, **4** (7) , 1146 (1994) .

73. A.F Denny , A.J Gioffre and J.D. Sherman , U.S. Patent N^0 4,094,778 , June 13 (1978) .

74. R. Le Van Mao , N.T. Vu , S. Xiao and A. Ramsaran ," Modified Zeolites Removal of Calcium and Magnesium from Hard Water " , J. Materials Chemistry, **4** (7) , 1149 (1994) .

75. J. Schafer and E. Stejskal , Journal of American Chemical Society , **98** , 1031 (1981) .

76. C.D. Chang , C.W. Chu and R. Socha , J. of Catalysis , **86** , 292(1984) .

77. R.A Llenado , Proc. 6th International Conference , Rena , USA , D.Olson and A. Bisio , Butterworth , Guildford (1984) .

78. S.J. Gregg and K.S King " Adsorption Surface Area and Porosity " Academic Press inc. , London , 140 (1982) .

79. R. Le Van Mao , S.T. Le , D. Ohayon , F.Caillibot ,L. Gelebart and G. Denes ; " Modification of the Micropore Characteristics of the Desilicated ZSM-5 Zeolite by Thermal Treatment " , Zeolites **19** (4) , 279 (1997) .

80. D.A Skoog " Principles of Instrumental Analysis " , 3rd ed. Saunders College Publishing , 464 (1985) .

81.J.W. Robinson , Analytical Chemistry , **32** , 17A (1960) .

82. D. Freude , "Studies of Surface Science Catalysis " , **52** , 169 (1989) .

83 . H. Kahn , Chemical Education , **43** , A7 (1966) .

84. M.E. Pillow , Spectrochem. Acta , **36B**, 821 (1981) .

85. A. Walsh , Pure and Applied Chemistry , **49** , 1621 (1977) .

86. R.D Dresser et al. , J. Chemical Education , **52** , A403 (1975) .

87. W.M. Meir and D.H. Olson in " Atlas of Zeolite Structure Types ", Butterworth-Heinemann , 3rd ed., London , 138 (1992) .

88.. Sie Ray 112 , X-RAY Diffractometer Automation System Software 2.1 , MD. USA .